Part VII
Case studies: industrial uses

36

INTRODUCTION

In many engineering uses of textiles the mechanical requirements are dominant. The designer is first of all concerned to ensure that the product has adequate strength. However, there are two difficulties; the loading conditions to which the material will be subject are often difficult to estimate, since they depend on the total dynamic response of the system in use; and the loading conditions which the material will withstand are difficult to calculate or measure, since they involve complex stresses acting on the fibres within the product. Consequently, most 'design' has been empirical, based on practical experience. There is, however, a growing need for a proper engineering design approach. A study of the ways in which products fail provides essential background information in this area.

We can revise Fig. 1.1 and present it in more specific form as Fig. 36.1, in order to show the lines of advance which are needed.

But apart from contributing to this long-term goal, the study of failure in textile structures used in industry and engineering is interesting, and can give short-term benefits. It can help the empirical design procedures, since when the mechanisms of failure are shown practical remedies may be suggested: modifying a structure to relieve stresses, adding a lubricant, changing the type of fibre, and so on.

Finally, particularly when there is litigation, it may be necessary to establish the cause of failure, and this can only be done when the different pathology of different causes of damage is established.

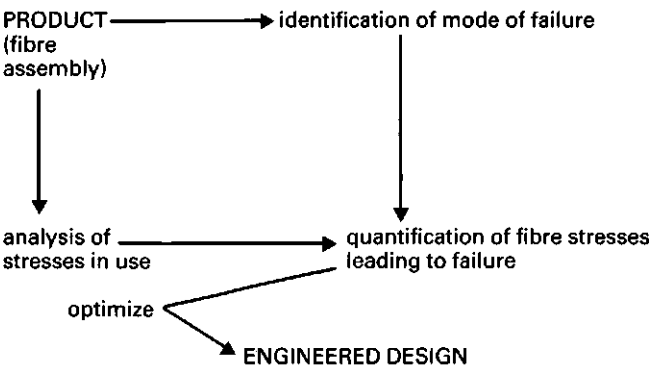

Fig. 36.1 — The route to fabric engineering.

37

AUTOMOBILE SEAT BELTS

I. J. Duerden

Seat belts are a protective device, but, in the rare circumstances in which they break, it is necessary to determine the cause of failure, in order to establish liability and to indicate how to reduce future accidents. However, before examining seat belts which have failed under service conditions, it is necessary to establish the forms of break which occur under controlled laboratory conditions. The following account is taken from work reported by Duerden, *et al.* (1983), of an investigation of new seat-belt webbing material which had been subjected to a variety of destructive loads.

Two types of material were used: nylon 66 and polyester. The construction of the webbing is essentially the same for both materials, although the description which follows is specifically that of the nylon webbing. The webbing, which is 5 cm wide, is made up of 264 warp ends; two of these are single-ply identifying ends, and the remaining 262 are two-ply Z-twist (2.5 t.p.i.) of 940 dtex continuous-filament yarn with 68 filaments per yarn. The filament size is 13.8 dtex or 12 den. Filling (weft) yarn is single-ply 940 dtex zero-twist continuous-filament yarn, again with 68 filaments per yarn. A 2×2 twill pattern is woven on a shuttleless loom with a lock-stitch of 555 dtex yarn, and there are 17 picks/inch. Reversing the twill pattern at intervals across the width produces panels. Use of a 2×2 twill increases the initial stiffness of the fabric over that of a plain weave. After weaving the webbing is dyed. The polyester webbing is also heat-set.

The webbing material used in this study of controlled fracture was first broken in simple tension. These tensile tests showed a mean failure load of 7040 lbf (31.3 kN) for nylon webbing and 6759 lbf (30.0 kN) for polyester webbing.

Samples of each type of webbing were broken in a variety of ways designed to simulate circumstances which might arise in service. It is appropriate to note that the macroscopic appearance of the fractured webbing is affected by the mode of failure, although what will be shown here are the fibre failures.

Webbing was failed in tension using a tensile testing machine fitted with grips which ensured failure due to tension. The approximate length of the webbing under tension was 50 cm and the extension rate was 25 cm/min. In practice seat belts seldom, if ever, fail in simple tension. Nevertheless, the appearance of fibres in webbing extended to failure in this manner provides a useful reference point.

The appearance of a nylon filament found in webbing failed in simple tension, **37A(1)**, is typical of the fibres found in this and similar specimens, and is a mushroom end, such as is found in single-fibre tests at high strain rates. This form results from rapid load transfer after break starts. Polyester fibres have a similar form in webbing failed in simple tension.

In actual service seat belts would be subjected to rapidly applied loads. To simulate this a drop test was devised. The webbing was used to arrest a 273-pound falling weight at decelerations of between 15 g and 35 g. In addition to the simple drop test, modifications were made to the test to simulate the effect of rapid loading on the webbing as it is pulled against either associated restraint system hardware (a D-ring, also known as a B-pillar swivel) or a sheet metal edge. The latter test was designed to assess the effect of intruding damaged vehicle parts on the webbing.

Both nylon, **37A(2)**, and polyester, **37A(3)**, filaments from webbing specimens failed in a drop test have an appearance similar to that of fibres found in specimens failed in simple tension, although the polyester end is somewhat more bulbous than that found on tension failure specimens. In polyester webbing which had been passed through a D-ring and drop tested, other effects of material melting may have occurred, **37A(4)**. At some places in the

webbing several filament ends could be seen to have fused together. A nylon filament, which formed part of a webbing specimen broken in a drop test over a sheet metal edge, is shown in **37A(5)**. The appearance of polyester filaments fractured in a drop test over a sheet metal edge, **37A(6)**, is characteristic of this type of failure mode. A similar appearance is found in some nylon fibres in webbing failed in this manner.

In service, seat-belt webbing is subjected to many forms of abuse. Perhaps the two most common are being dragged along outside a vehicle and being repeatedly trapped between the door and the door frame of a vehicle. To simulate this latter phenomenon a sample of webbing was folded perpendicular to its length and then struck repeated blows with a hammer along the fold while lying on an anvil. Beating was continued until the webbing separated. The resulting fibre failure morphology is illustrated in **37B(1)**.

The ageing of webbing samples was simulated, by exposure to ultraviolet radiation, in order to determine the effect of weathering upon mechanical properties. Three levels of exposure were used: 100, 200 and 300 hours. After exposure the webbing was broken in simple tension and the failure morphology examined. The effect of 300 hours exposure upon the failure morphology of nylon is illustrated in **37B(2)**. There is also an effect upon the macroscopic appearance of the webbing, particularly in the case of nylon, where the extent of the damage associated with tensile failure is dramatically reduced by exposure to ultraviolet radiation. The reduction in strength concentrates the zone of damage imposed by the breaking load.

On occasion, webbing is deliberately cut by rescue personnel, and it is important to be able to identify webbing which has been separated in this manner. A polyester filament in a webbing specimen cut with a pocket knife, **37B(3)**, has a fan-like appearance. This effect is typical of a knife cut, and is seen in nylon as well as polyester webbing. A sharply defined flat surface is found in a nylon filament from a webbing cut with a scalpel blade, **37B(4)**. The striations on the surface correspond to fine grinding marks on the blade. The fracture morphology in the nylon fibre, **37B(5)**, is typical of that produced by a scissor cut of webbing. Polyester filaments exhibit a similar form. Not all scissor cuts produced this appearance; some were more like the fibres illustrated in **37B(6)**, which is a polyester filament from a webbing cut by tin snips (metal shears). Note that there is no evidence of pinching, as is seen in other examples of scissor cuts. This form of failure appears in both nylon and polyester webbing.

In the remainder of this Chapter we show illustrations of the failure morphology of webbing which has broken in service. The circumstances surrounding each failure are outlined and conclusions are drawn from examination of the photomicrographs. A report on some of these failures has been given by Duerden and Dance (1984).

The first pictures are from the driver's seat-belt webbing in a vehicle which skidded sideways into the rear of a parked vehicle. Extensive damage occurred to the driver's side (left-hand side) of the skidding vehicle, the maximum intrusion into the vehicle in this region being 38 cm. Examination of both the macroscopic and microscopic appearance of the separated webbing indicated that failure was due to a combination of tensile loading and cutting of the webbing by intruding sheet metal edges which resulted from the collision. Two representative failure morphologies found in the webbing are presented. The fibre shown in **37C(1)** has an appearance typical of many fibres in this sample. Mushroom end failures such as this are a consequence of tensile overload. The failure morphology exhibited by the fibre illustrated in **37C(2)** shows distinct evidence of a shearing action consistent with the fibre being pulled across a metal edge, and may be compared with **37A(5)**.

In the second accident a vehicle was involved in a head-on collision with a small truck. There were five occupants in the vehicle: two in the front who were wearing seat belts and three in the back who were not restrained. The three rear seat occupants were thrown forward upon collision into the back of the front seats. Examination of the webbing and restraint system hardware produced evidence that the webbing had developed a fold along its length and became trapped in the D-ring. Samples of seat-belt fibre were found trapped in the D-ring slot. This hypothesis is also supported by the microscopical appearance of failed fibres found in a narrow zone in the region of the fold crease on the webbing.

The general appearance of fibres in the suspect zone of the webbing shows several different failure modes, **37C(3)**. More detailed examination illustrates a morphology typical of tensile failure accompanied by crushing, **37C(4)**, which is consistent with the fibres having been pulled over a metal edge, **37C(5)**. Two other morphologies can be seen in **37C(6)**, namely a pinching/cutting type and a high-speed tensile failure in the rear.

In another accident the webbing failed in a high-speed roll-over collision in which the passenger wearing the seat belt was ejected from the vehicle. Two separate failure zones were identified by visual examination: one suggested that simple tensile failure had occurred and this was confirmed by scanning electron microscopy; the appearance of the other zone suggested that the material may have been cut. Examination of this region in the SEM showed that the fibres had been crushed. The appearance, **37D(1)**, is consistent with the webbing being damaged prior to the accident by being jammed between the door and the door frame. A comparison may be made with **37B(1)**. It was concluded that failure occurred because of the prior damage in this zone.

It is not too uncommon to find seat belts which have been chewed by a dog. An example from the nylon belts examined in Canada is shown in **37D(2)**. Some other examples from a

sample submitted to UMIST by the Royal Aircraft Establishment (RAE) are shown in **37D(3)-(6)**. Most of the seat belt was undamaged, and the nature of the fabric is shown in **37D(3)**. This appearance was typical of most of the material, with little sign of wear and only slight contamination by dirt particles. However, there were two distinct regions of damage, and, in one of these, the belt had been completely severed. The two regions were about 60 mm apart, which is probably the bite width of the dog.

The edge of the severed region, **37D(4a)**, shows the broken fibre ends and the disturbance of the fabric by the chewing. Individual fibre ends, **37(4b),(5)** have flattened wedged-shaped ends, which result from the sharp biting (cutting action). There are signs of damage further back along the filaments, which are distorted and often bent back, **37D(6)**.

1 20 μm

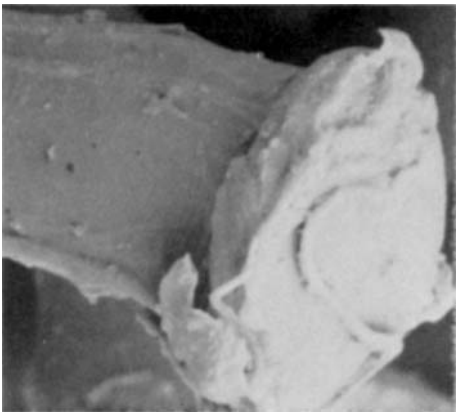

2 10 μm

3 20 μm

4 20 μm

5 10 μm

6 20 μm

Plate 37A — Laboratory tests of automobile seat-belt webbing.
(1) Nylon filament from webbing broken in tensile test. (2) Nylon filament from webbing broken in drop test. (3) Polyester filament from webbing broken in drop test. (4) Polyester filament from webbing failed in drop test with D-ring. (5) Nylon filament from webbing broken in drop test over sheet metal edge. (6) Polyester filament from webbing broken in drop test over sheet metal edge.

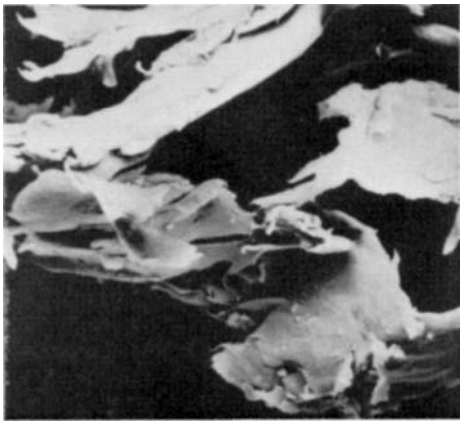

1 ⟷ 20 μm

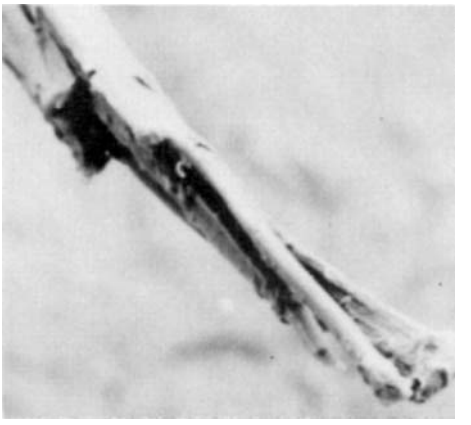

2 ⟷ 20 μm

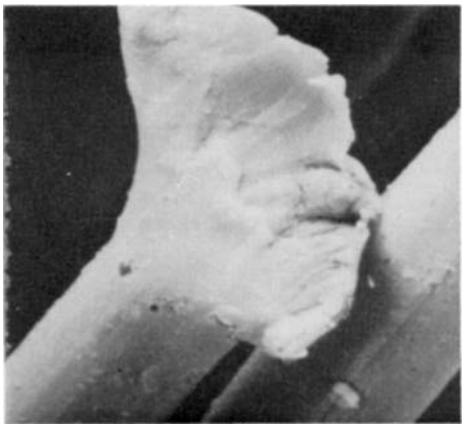

3 ⟷ 10 μm

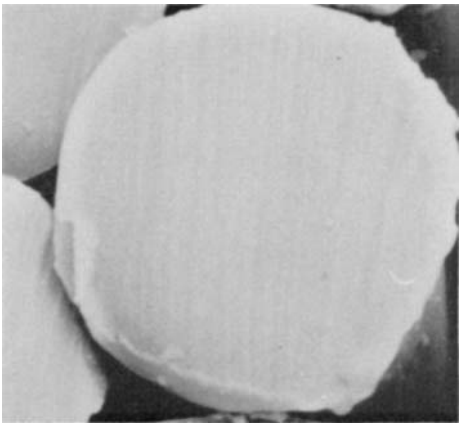

4 ⟷ 5 μm

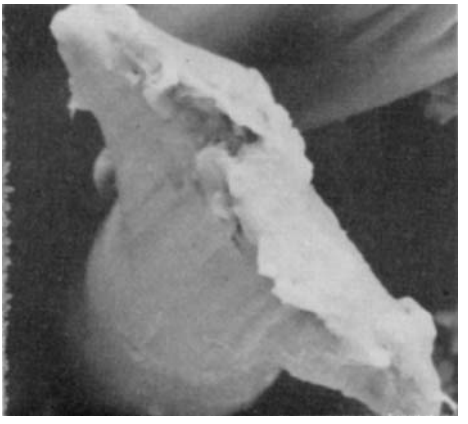

5 ⟷ 10 μm

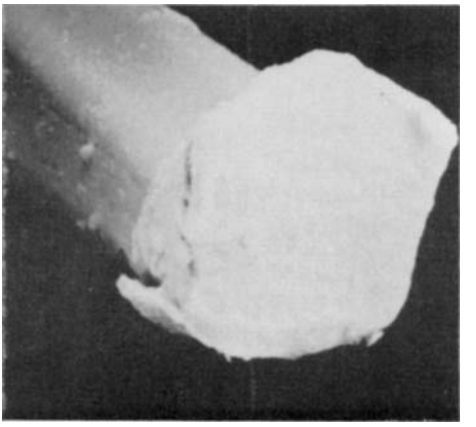

6 ⟷ 10 μm

Plate 37B — Laboratory tests of automobile seat-belt webbing (continued).
(1) Nylon filament from webbing broken by repeated pinching between a hammer and an anvil. (2) Nylon filament from webbing failed in tension after 300 hours exposure to ultraviolet radiation. (3) Polyester filament from webbing cut with a knife. (4) Nylon filament from webbing cut with a scalpel. (5) Nylon filament from webbing cut with scissors. (6) Polyester filament from webbing cut with tin snips (metal shears).

1 ⊢⊣ 10 μm

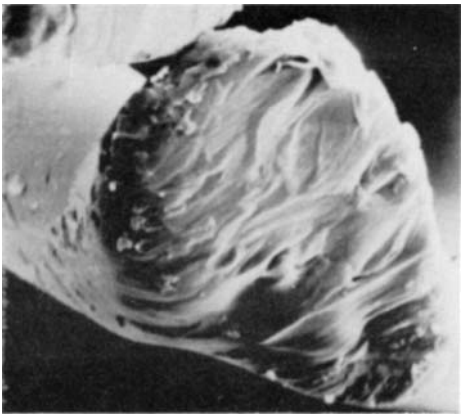

2 ⊢⊣ 10 μm

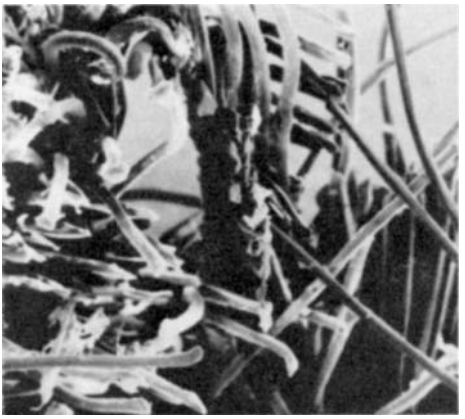

3 ⊢⊣ 20 μm

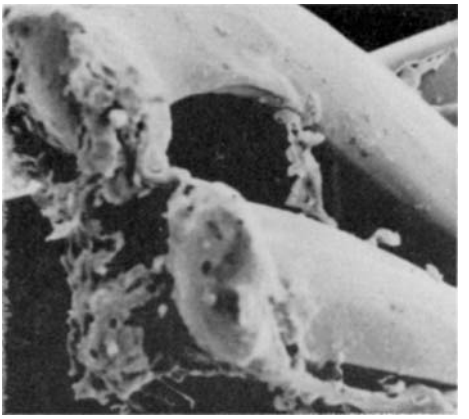

4 ⊢⊣ 20 μm

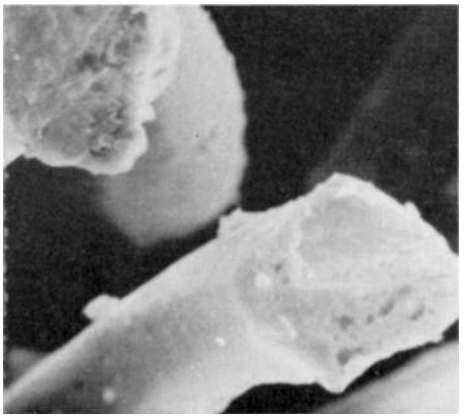

5 ⊢⊣ 10 μm

6 ⊢⊣ 10 μm

Plate 37C — Seat belt from a skidding accident.
(1),(2) Failed polyester fibres from the broken webbing.
Seat belt from a head-on collision.
(3) Fibres in suspect zone of webbing, at a fold trapped in a D-ring. (4)–(6) Details of fibre failure.

1

2 50 μm

3 2 μm

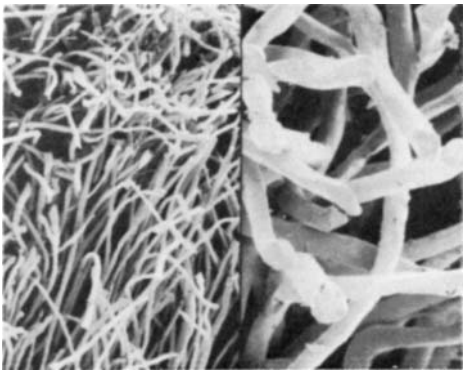

4a 500 μm 4b 100 μm

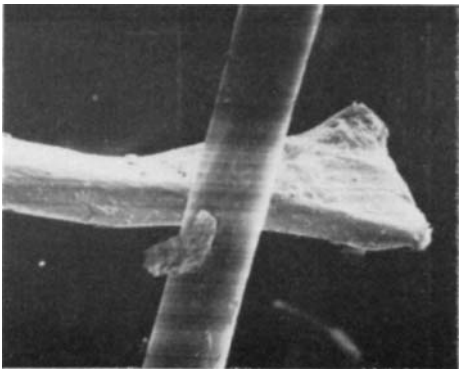

5 20 μm

6 100 μm

Plate 37D — Seat belt from a high-speed roll-over collision.
(1) Nylon fibre failure.
Seat belt chewed by a dog (Canadian study).
(2) Damaged nylon fibres.
Seat belt (nylon) chewed by a dog (RAE).
(3) Fabric from surface of belt, in a region which has not been chewed. (4a) Fabric at edge, which has been chewed through. (4b) Detail of fibre ends. (5) Severed fibre. (6) Material in chewed region.

38

MILITARY WEBBINGS AND CORDS

Narrow woven and braided materials are used in a wide variety of applications as fasteners and connectors. Depending on their shape and end-use, those of medium size are usually known as webbings or cords. They are found in many places in military equipment, and the case studies reported in this chapter have come from RAE, Farnborough.

The first example is the retraction strap of the ejector seat on a Jaguar aircraft. This was a continuous-filament nylon woven webbing, but had developed a hairy surface owing to projecting loops and broken filaments. Wear was particularly severe on the inner curved edge of the strap, and was probably associated with friction between the strap and the clip through which it slides.

Broken yarns at the badly worn edge of the strap are shown in **38A(1)**. The early stages of filament breakdown suggest a combination of multiple splitting due to flexing and peeling caused by surface shear, **38A(2)**. Some broken fibres have bushy ends, **38A(3)**, which could be due to biaxial rotation fatigue (Chapter 13), but the absence of indications of twist suggest that simple flex fatigue (Chapter 12) may be the cause. Alternatively, other filaments have flattened and mangled ends, **38A(4)**, presumably due to a shearing or cutting under high normal loads from the guide.

Where weft yarns have been severed, they shrink back into the fabric, **38A(5)**. Examination of broken filaments, **38A(6)**, shows flat ends which are sheared in one direction and subdivided into many zones. This suggests that they had first split and then been sheared off or, less likely, been gradually worn smooth.

The second set of examples result from a very different wear environment: they are webbings from arrester harnesses on airfields. Detailed study showed interesting differences between different parts of the webbings, but only some common features will be described here. Surprisingly, webbing which had been used for 12 months on a concrete surface, **38B(1a)**, showed less damage than one which had been used for only 4 days, **38B(1b)**. This presumably reflects the irregular usage of such equipment. The comparatively minor wear after long use occurs on the yarn crowns, where there is a smearing over the surface, **38B(2)**, as a result of material being peeled off, **38B(3)**. The peeling action on the 4-day specimen is more drastic, **38B(4)**, giving a very ragged appearance with some material rolled up. Other regions of the webbing are hairy owing to filament breakage, **38B(5)**, with evidence of multiple splitting, **38B(6)**.

Webbing which had been used for 12 months on a tarmac surface had also been scraped and smeared, **38C(1)**, with some material being rolled up, **38C(2)**. Detailed views show how a substantial part of a filament can split off and roll up, **38C(3),(4)**. Other parts of the webbing showed less severe damage by smearing, **38C(5)**, or an absence of wear but considerable contamination by debris, **38C(6)**.

Equipment used on airfields suffers damage not only through general mechanical wear and environmental degradation and emergency overloads, but also through extraneous causes. For example, **38D(1)** shows an arrester barrier centre marker after it had been damaged by rabbits. The teeth marks can be seen in the plastic-coated fabric. Where the material has been bitten through, **38D(2)**, the fibre ends are flattened into a spatula shape, **38D(3)**. Other fibres show damage over a greater length, **38D(4)**, and were probably broken by abrasive action, rather than being directly cut by the action of the teeth.

In contrast to this a webbing which has been cut with a file shows a different type of damage, **38D(5)**. Adjacent to the severed region, the filament tips are bent over, **38D(6)**, indicating the direction of movement of the file.

The next example is again wear due to normal use, and consists of two nylon border cords from cargo nets used in helicopter supply operations. The cord is a hollow circular braid, which

has flattened into a webbing about 8 mm thick. The surface of the cord had been treated with a dark grey coating, which held the filaments together. One sample had only very slight damage, as can be seen from the appearance of the surface, **38E(1)**, although there are a few broken filaments on the edges of the cord, **38E(2),(3)**. The flattened and distorted appearance of the filaments indicates that breakage was due to heavy lateral pressure. The second sample was much more severely worn, and the colour had changed from dark grey to a light silver. The surface of the cord is badly disturbed, **38E(4)**, and on one edge the filaments were twisted and tangled, **38E(5)**. The fibre breakage, **38E(6)**, again appeared to result from the lateral pressure.

The last example is of parachute rigging lines, which are nylon braids. The material had suffered damage which led to the appearance of pairs of small fluffy knobs about 1 cm apart, which were the two broken ends of twofold continuous-filament yarns. A broken end extracted from the fabric is shown in **38F(1)**. The individual filaments give evidence of considerable squashing and splitting, with adhesion by softened material, **38F(2)**, and some broken ends have a complicated mangled shape, **38F(3)**, although others, probably among the last to break when they were taking a high load, are mushroom ends, **38F(4)**, similar to those found in high-speed breaks.

Another rigging line showed more widely distributed fibre damage, **38F(5)**, with evidence of high lateral pressures, **38F(6)**.

Among the samples which came to us from RAE was an interesting example of wear in flax, used in restraint webbings related to ejection by aircrew. The general damage, **38G(1)**, shows the typical wear found at the interstices between yarns in woven and braided fabrics. Squashing, **38G(2)**, possibly by webbing hardware, and fibrillation, **38G(3),(4)**, are two ways in which the flax fibres are damaged. However, a novel feature of deformation in flax fibres, which may also occur in other similar plant fibres, is sharp bending at nodes, as seen in the bottom right corner of **38G(4)**. These open into cracks, **38G(5)–(7)**. The break in the middle of **38G(4)** probably occurred at such a node and was accompanied or followed by some axial splitting.


1 200 μm

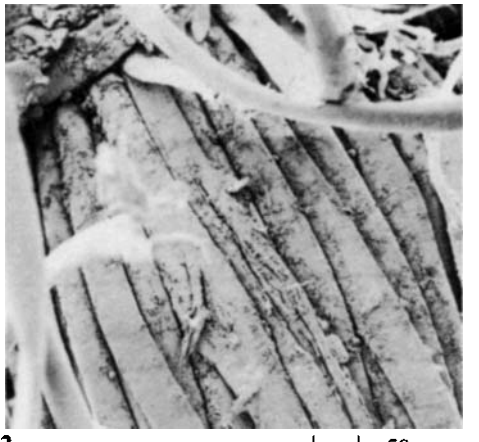
2 50 μm

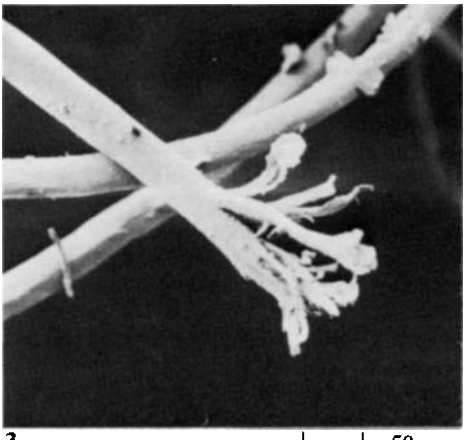
3 50 μm

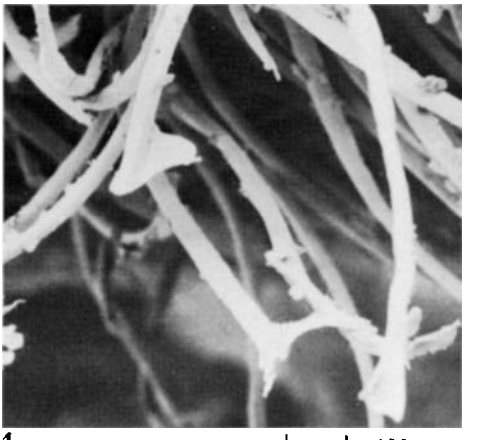
4 100 μm


5 500 μm


6 50 μm

Plate 38A — Worn nylon strap from Jaguar aircraft ejector seat.
(1) Severely worn yarns at edge of strap. (2) Detail of badly worn area. (3),(4) Broken filaments from worn area. (5) Several yarns: note broken end of yarn pulled back into fabric, near bottom right corner. (6) Detail of broken yarn.

1a 1 mm 1b 1 mm

2 100 μm

3 50 μm

4 100 μm

5 1 mm

6 50 μm

Plate 38B — Nylon arrester harness used on concrete runway.
(1a) Surface after use for 12 months. (1b) Surface of another webbing after use for 4 days. (2), (3) Wear on 12-month specimen. (4) Wear on 4-day specimen. (5),(6) Selvedge region of the 12-month specimen.


1 1 mm


2 100 μm


3 20 μm


4 50 μm


5 100 μm

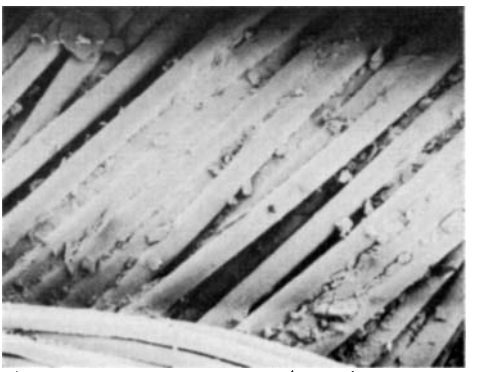
6 100 μm

Plate 38C — Nylon arrester harness used on tarmac for 12 months.
(1),(2) Wear on surface. (3),(4) Detail of fibre damage. (5),(6) Other parts of the webbing.

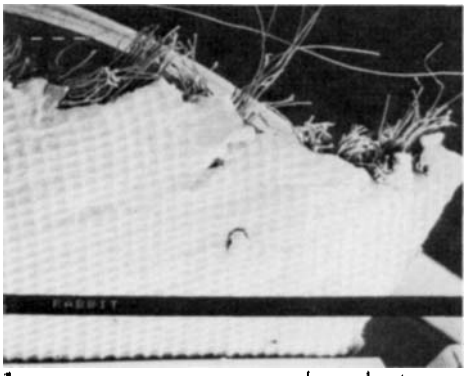

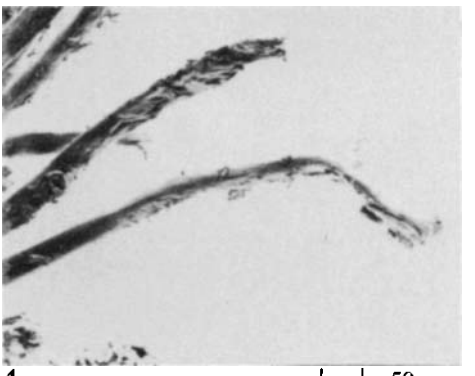

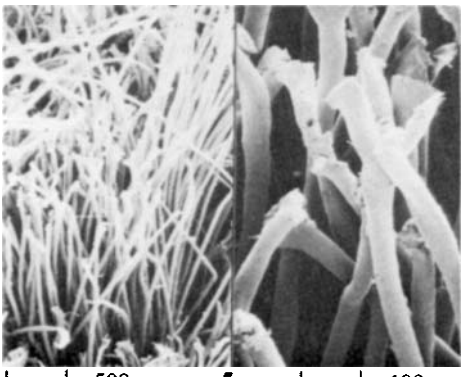

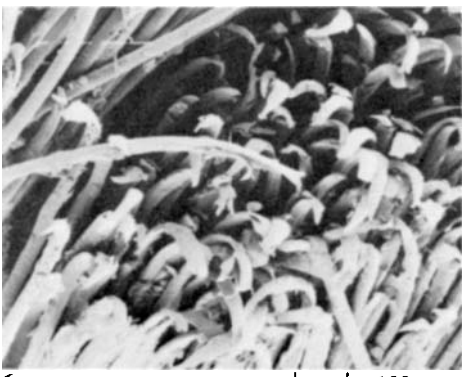

Plate 38D — Nylon arrester barrier centre marker damaged by rabbits.
(1) General view. (2) Detail of bite. (3) Fibre end from bite. (4) Other broken fibres.

Nylon webbing cut with file.
(5) Cut region. (6) Adjacent to cut.

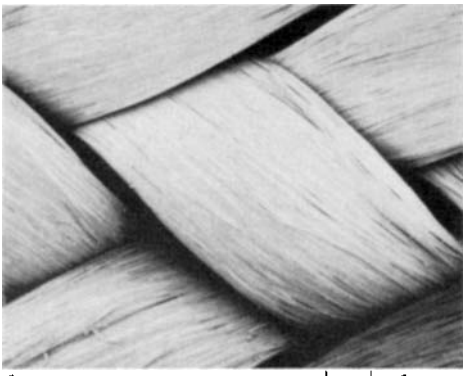
1 1 mm

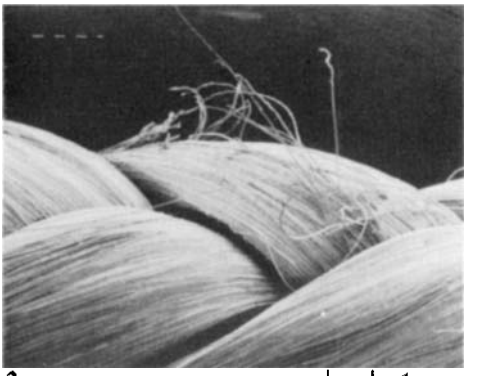
2 1 mm

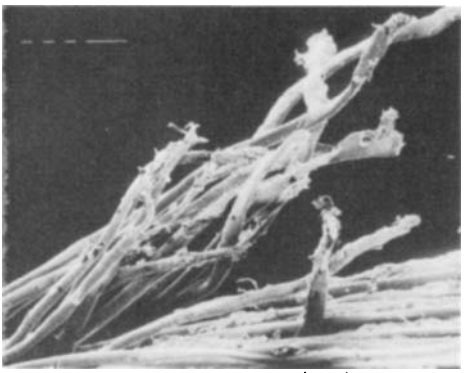
3 100 μm


4 1 mm

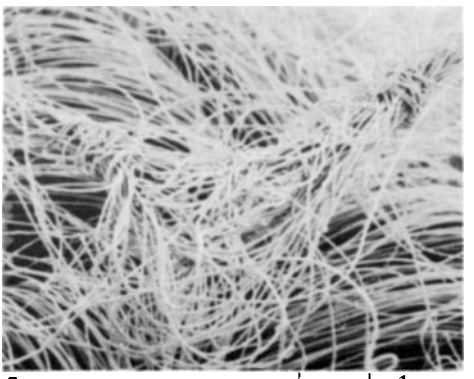
5 1 mm

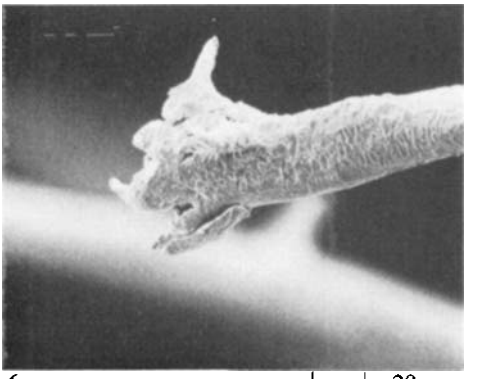
6 20 μm

Plate 38E — Nylon border cords from helicopter cargo nets.
(1) Main surface of little-worn cord. (2) Edge of little-worn cord. (3) Detail of fibre breakage. (4) Main surface of severely worn cord. (5) Edge of severely worn cord. (6) Detail of fibre breakage.

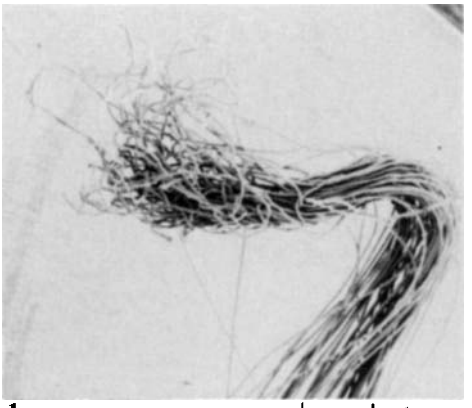

1 1 mm

2 50 μm

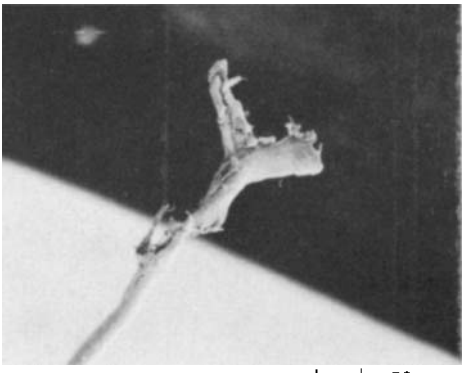

3 50 μm

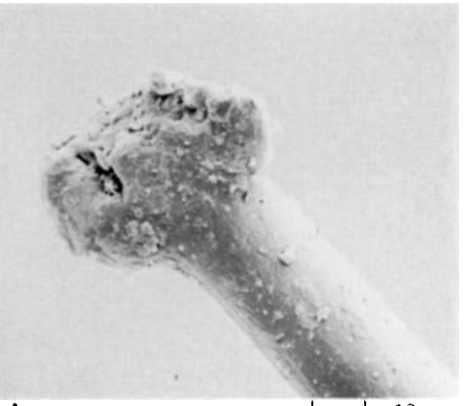

4 10 μm

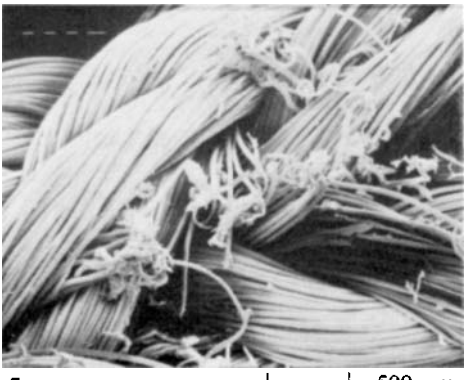

5 500 μm

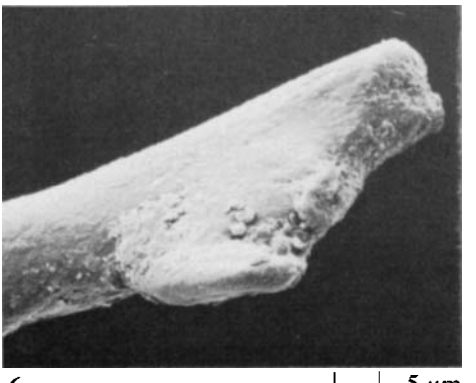

6 5 μm

Plate 38F — Nylon parachute rigging line with localized yarn breakage.
(1) Broken yarn end, removed from the braid. (2) Fibre damage. (3),(4) Broken fibre ends.

Another rigging line.
(5) General view of wear. (6) Broken fibre.

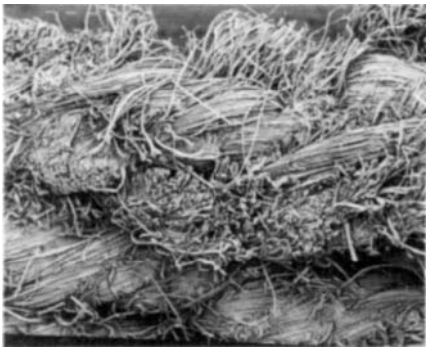

1

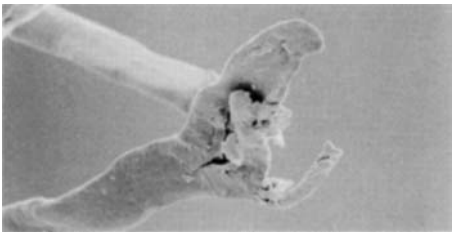

2

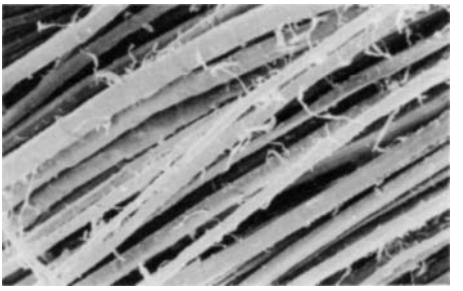

3

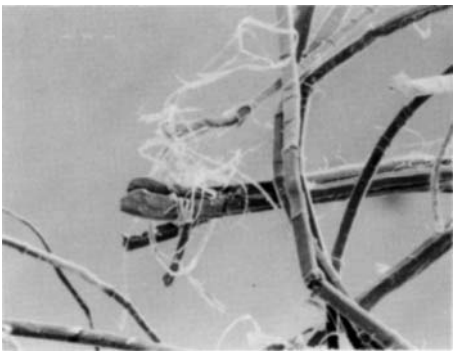

4

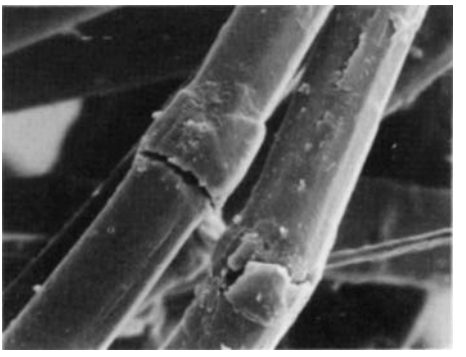

5

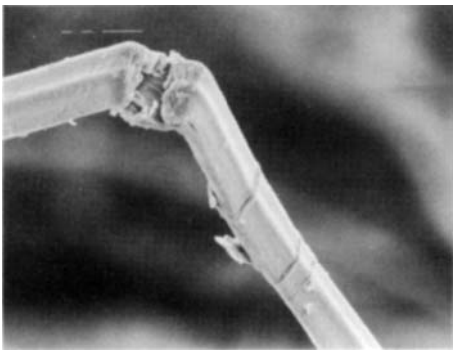

6

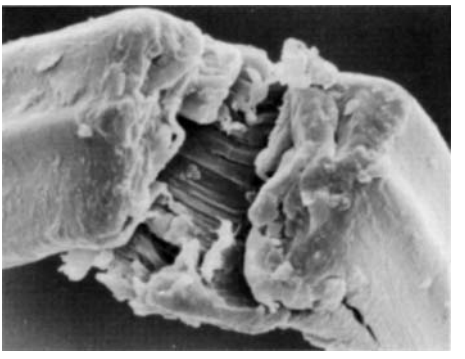

7

Plate 38G — Wear of flax restraint webbings.
(1) General damage. (2) Squashed fibre end. (3) Fibrillation. (4) A variety of forms of damage. (5)–(7) Cracks from bends at nodes.

39

ROPES

Ropes provide examples of interesting forms of fibre failure, particularly associated with abrasive wear both on the surface of the rope and between fibres within the rope.

It has recently been found in studies by a number of investigators that nylon ropes break down rather rapidly when exposed to repeated loading in a marine environment. Although nylon products usually show excellent durability in dry conditions, moisture absorption causes changes in properties. In some single-fibre fatigue tests, involving bending and twisting, this may increase life; but in surface abrasion resistance the performance of wet nylon is poorer than of dry nylon. In contrast to this, polyester fibres with much lower moisture absorption show good abrasion resistance, both wet and dry.

As an example, taken from OCIMF tests, **39A(1)** shows a large nylon rope which had broken after being cycled wet between a low load and 50% of its single-test breaking load: under the repetitive loading the rope lasted for only 970 cycles. A polyester rope would have lasted for millions of cycles at this loading, and would have needed a loading of around 90% of its normal breaking load to fail in less than 1000 cycles. In the nylon rope the original continuous filaments had broken down into short fibres, as a result of a splitting and peeling shown for a collection of fibres in **39A(2)** and in more detail in **39A(3)–(6)**.

The next example comes from a failure in use of a rope, which was then subjected to very detailed examination. The rope was a nylon rope which was used to tie the skirt of a hovercraft onto the vessel itself. Failure was occurring after a short period of use, and it was found that the problem was that a cheaper nylon rope had been substituted for the previously used polyester rope. A return to the earlier practice solved the problem.

A length of the nylon rope, removed because it was near to failing, is shown in **39B(1)**. Some parts of the rope were almost undamaged, **39B(2a)**, apart from slight surface rubbing, a few broken filaments and some contamination with dirt; other parts showed clear evidence of moderate wear, **39B(2b)**; and near the knot in the eyelet of the skirt, the rope had almost broken, **39B(2c)**.

SEM study of the least worn rope surface, **39B(3)**, shows the contaminating particles jammed between the filaments, together with some rubbing wear on the fibre surfaces. The broken filaments have bushy ends, **39B(4)**, in which the fibrillar splitting has developed from one side, presumably due to layers peeling away as a result of abrasion. In the moderately damaged region there are many more broken filaments, but these have the same form of break, **39B(5)**. Close examination of this picture shows that the breakdown into the fine fibrils of bushy ends follows the peeling away of successive layers of material. An early stage of peeling from a fibre surface is shown in **39B(6)**, which also illustrates the varied nature of the contamination with some rounded granular particles and some cubic salt crystals.

In the badly damaged region near the knot, the structure is extremely complicated, **39C(1)**: there are some fibrillated broken ends, but other fibres show contortions characteristic of snap-back after rapid break, and there are some signs of lateral pressure.

Surface wear can be expected in a rope and, if the main body of the rope is intact, does not cause serious weakening. It is therefore necessary to look for damage within the rope. Because of the great confusion in the region of worst damage, it is best to start with the least damaged part, **39C(2)**, and look for wear between the strands. There is clearly appreciable damage to the fibres, **39C(3)**, where the strands rub against one another under the lateral pressures within the twisted rope. Layers are peeled off the filaments, and tend to group together to give a tide-mark, **39C(4)**. Examination of individual fibres shows the peeling of separate layers, **39C(5)**, which then fibrillate. The peeling goes progressively deeper into the fibre until there is breakage, as shown respectively by the upper and lower fibres in **39C(6)**.

The mechanics of failure can be expressed in the following terms. The rope as a whole will

undergo repetitive tensioning, owing to the interaction of the vessel, the skirt and the sea, with possibly some bending or twisting. Within the rope there will be inter-strand movement and lateral pressure, which will generate frictional forces between the fibres. Material near the fibre surface will thus be subject to reciprocal shear forces, which cause the layers to peel away, as discussed in Chapter 14. Further rubbing will split the layers into fibrils.

Having established the essential nature of inter-strand wear, it is necessary to examine more severely worn regions to confirm that the same mechanisms are operative. In the moderately damaged region the effects are seen to be similar, but much more pronounced, in **39D(1)**. The yarn surfaces near the centre of the picture have been worn smooth; further out the tide-marks of peeling can be seen; and, at the outer edges of the picture, there are the fibrillated ends of broken filaments. Near the surface of the rope individual broken filaments show the characteristic bushy end, in an extreme 'mop-head' form, **39D(2)**. Within the strand there is considerable filament splitting, **39D(3)**, but the ends are not as bushy and often taper owing to the removal of successive layers.

Examination of the most severely damaged region is difficult because there is so much fibre breakage that the rope structure has become much looser. However, the same form of fibrillated breaks can be observed, and the peeling may occur over long fibre lengths, **39D(4)**. Some fibre breaks are typical tapering ends, **39D(5)**, but others show little sign of peeling and are probably caused by one filament cutting through another, **39D(6)**, under high lateral pressure.

Although the rope and strand surfaces are the most prone to damage, wear also occurs deeper within the rope structure. In the least damaged region inner ply yarns showed kinking and the beginning of surface peeling, **39E(1)**. A closer view of the peeling on the inner surfaces of singles yarns within the rope is shown in **39E(2)**. The surface appearance of the fibre in **39E(3)** suggests that inter-fibre adhesion may have occurred, with the subsequent separation loosening minute portions of the fibre surface. This would later lead to peeling, **39E(4)**.

Fairly severe peeling can be found in the inner surfaces of outer ply yarns, **39E(5)**. In a more severely damaged part of the rope, **39E(6)**, there is kinking of filaments and contamination with particles, which are probably salt crystals.

The next example comes from an extremely demanding rope use: a kinetic energy recovery rope (KERR). In this application the nylon rope is used to pull out a military vehicle when it has got bogged down. The extension of the rope stores up elastic energy, which is then available to continue the pull once the vehicle starts to move. During the operation much heat is generated, and it is usual to find that the ropes will not survive many periods of use.

Strands removed from positions away from the point of break in two failed ropes were examined, and are illustrated in **39F(1)**. The fusing due to heat is very clear, but is strictly localized, with a sharp transition to regions where the fibres are little damaged. Some individual breaks show projecting tails, **39F(2)**, perhaps where softened material has been pulled away, but others show a multiplicity of such effects, **39F(3)**. Particularly in regions of snap-back, heat has caused the fibre surface to become wrinkled, **39F(4)**. The appearance of the interior, seen through cracks in the skin, suggests that the inside of the fibre had become molten, **39F(5)**, and, in a severe case, the molten material had burst through the skin, **39F(6)**.

In the KERR and many other rope uses, damage may be caused either by the action of heat or by mechanical action. In order to investigate the effect of heat alone, H and T Marlow Ropes carried out a set of tests in which they heated ropes to 160°C for 33 hours, and then carried out a tensile test either at the elevated temperature or after cooling down to room temperature.

As a result of the heating, polyester ropes had changed to a pale cream colour. Failure of one rope in the tensile test had resulted in two strands breaking, with considerable recoiling on one side of the break but not on the other; the third strand had not broken. Heat is generated by the sudden release of energy on rupture, and fusing was apparent in many places, including the surface of both the unbroken strand, **39G(1)**, and the broken strands, **39G(2)**. There is also fusing at broken yarn ends. For inner yarns the fusing is moderate in extent, **39G(3)**. The ends of broken filaments tend to thicken towards their tips, in some instances, then tails project from the broken ends, **39G(4)**, presumably of softened material drawn out at the moment of rupture. Where the filaments are free, and not fused, mushroom-shaped ends characteristic of high-speed break are observed, **39G(5)**. In outer yarns the fusing is more severe, **39G(6)**.

Nylon 6 ropes show greater discoloration as a consequence of the heat treatment: they are generally deep gold, but near the break are dark brown or almost black. In the rope subsequently tested at room temperature all three strands had broken, but in the rope tested hot only two of the strands had broken. There is no fusion between the rope strands or ply yarns within the strands, and the broken yarn ends showed no entanglement.

In the rope broken hot, rupture had occurred by breaks which run sharply across the yarn, **39H(1)**, although closer examination shows that this is in separate steps, **39H(2)**. The main cores of the fibres show a granular break, **39H(3)**, which is typical of the effect of thermal degradation on nylon. There appears to be a different skin layer; and on each fibre the break fans out from a point of contact with a neighbouring fibre. This suggests that there is fusion or very intimate contact between fibres, so that the break can propagate from one fibre to another.

In the rope broken at room temperature the form of breakage is similar in inner plies,

39H(4), except that the individual fibre failure commonly occurs in V-shaped ridges, **39H(5)**, which are along the lines of high shear stress. In outer plies, where lateral pressures have been less, the filaments break at different locations across a yarn, and different forms of fibre break are seen. Sometimes there are transverse granular breaks, but where filaments have fused together failure may be at an angle owing to shear stress, **39H(6)**.

Finally, we show some miscellaneous examples of rope failures. In a Kevlar yachting rope, used for a Genoa sheet, the failure shows the fibrillation which is characteristic of Kevlar, **39I(1)**, but the damage is clearly intensified by the presence of salt crystals, **39I(2),(3)**.

The other examples were supplied by RAE, and show rather different forms of damage.

The first was a nylon rope used in mountain rescue work. The rope had been badly scuffed and abraded, and was covered with fibre fragments and other debris. There was damage to filaments by peeling, and broken ends were flattened and distorted, **39I(4)**, owing to the scraping and abrading in use.

The second, a polypropylene rope used to tow gliders, was also severely worn. The filaments had split into ribbons of various widths, **39I(5)**, so that the appearance at different magnifications was similar. Where the damage had led to filament breakage this was in the form of long multiple splits, similar to those found in flex fatigue.

The third was a nylon aircraft barrier rope. This showed localized damage, with severing of yarns in places along the rope, presumably due to high impact loading. Broken filament ends were ragged, smeared and misshapen. There was fusing together of filaments, **39I(6)**, indicating considerable frictional heating.

39J(1),(2) shows the breakage of a filament taken from the outer surface of a 3-strand nylon mooring line, which had been manufactured at Boston Naval Shipyard and used for several years. This comes from an extensive research programme at MIT, reported by Backer *et al* (1983), Backer and Seo (1985) and Seo (1988), which included the pathology of worn US Navy and Coastguard ropes. The rupture has the stake-and-socket form, which has previously been observed in degraded polyester fibres, **16D(1),(2)** and **34G(4)–(6)**, and in hair, **19D(2)–(4)**. In this example it is a consequence of photo-degradation of nylon.

Natural fibres are now less used in ropes, but **39J(3)–(6)** and **39K** are pictures of a flax rope from RAE. This is interesting as showing how flax fibres break. A laboratory break test of an unused rope is relatively sharp, though it divides into separate bundle breaks and there is some structural disturbance. Some fibre breaks appear to be granular tensile breaks, **39J(3)**, but others show more splitting, **39J(4)**. There is also evidence of breaks at kink-bands, **39J(5)**, which may result from snap-back and may be at nodes similar to those seen in **38G(6),(7)**. Higher magnification views of the detail of failure within a flax fibre show the separate rupture of the ribbons of cellulose fibrils, **39J(6)**. In a used rope, wear seen on the rope surface in **39K(1)** comes from external abrasion. As it becomes more severe, strands break irregularly, **39K(2)**. There is considerable disarrangement of fibres, **39K(3)**, which in places form entangled balls. Breakage of individual flax fibres shows splitting and smearing, **39K(4),(5)**, though some individual breaks, **39K(6)**, are cleaner and more like those found in the laboratory break test.

Polyester ropes last longer under fatigue in wet conditions than nylon ropes which fail by internal abrasion as illustrated in **39A–E**. Even where two polyester strands come together within a sub-rope in a multi-strand rope, there is very little sign of wear, **39L(1)**. This is where a nylon rope would show severe wear, as in **39C(3)**. Although the polyester had been out in a sea-trial of a mooring for a considerable time, hardly any damage is apparent. In some parts of the rope, **39L(2)**, there was an accumulation of debris, which has led to slight peeling. The occasional broken ends have failed along kink-bands, **39L(3)**, sometimes associated with axial splitting, **39L(4)**, or have been squashed, **39L(5)**. The jacket suffers more damage due to external abrasion, as shown in **39L(6)**, with a higher magnification picture as **39L(7)**, showing a fibre bent at two or three places, leading to cracks and then rupture at the most severe damage location.

A large number of small ropes made from different high-performance fibres in a variety of rope constructions were subject to tension–tension fatigue in a joint industry study, FIBRE TETHERS 2000 (1995), aimed at the evaluation of fibre ropes for deepwater moorings. The commonest damage mechanism was axial compression fatigue, which occurs when a rope component goes into compression, even though the rope as a whole is always under tension. The compression results either from twisting of the rope or from differential lengths of rope components.

An analysis by Hobbs *et al* (1997) showed that the mechanics of deformation was similar to that in the buckling of heated pipelines on the seabed. The factors involved are: (i) development of an axial compressive stress along a length of the component; (ii) axial slip against friction; (iii) buckling giving a lateral displacement opposed by restraining forces. The analysis showed that this results in groups of buckles at intervals along the component, separated by straight portions. In the elastic deformation of the pipleline, the buckles are sinusoidal waves, but, in the elastic–plastic mode of yarn or fibre bending, sharp kinks

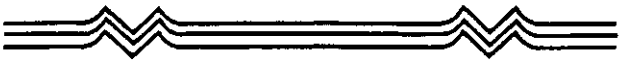

Fig. 39.1 — Predicted form of buckling of fibres and yarns due to axial compression within a rope. There is a set of solutions with different numbers of kinks between straight parts.

develop. The form of the predicted kinking is shown in Fig. 39.1. The kinks then lead to the yarn breaking into short pieces, separated by longer unbroken lengths.

This theoretical prediction is confirmed by fatigue tests on small ropes with a break load of about 5 tonnes. **39M** shows pictures from the central yarn of a Kevlar aramid rope after tension–tension cycling, in which this yarn will have been subject to axial compression, As the core strand is opened up, **39M(1)**, broken pieces can be seen and, back along the yarn from the last break, a kink, which has started to fail. Similar effects are visible in the extracted length of yarn, **39M(2)**. Examination of fibres by optical microscopy shows kink-bands within straight portions of fibres due to axial compression, **39M(3),(4)**, which can join in pairs and project out of the fibre surface. The axial slippage referred to above can lead to a concentration of kink-bands, **39M(5)**. A sharp kink in a whole fibre and some axial splitting is shown in **39M(6)**. Break at a kink in a fibre is seen in **39M(7)**. Fibre breaks usually run across the fibres at 45°, **39M(8),(9)**, but sometimes with complications, **39M(10)**. An unusual break at a sharp angle across the fibre is shown in **39M(11)**. A more usual break along the typical angle of approximately 45° of a kink-band is shown in the SEM picture, **39M(12)**. A break at a kink in a fibre with some axial splitting is shown in **39M(13)**, which has similarities to **39M(7)**. In **39M(14)**, several pairs of kink-bands can be seen projecting at 90° to each other on the surface of the fibre below the break. The break itself has developed by cracks along a similar pair of kink-bands, with some disturbance due to splitting. A longer axial split is associated with the break in **39M(15)**.

Kinks at intervals along a yarn in a Twaron aramid rope after tension–tension fatigue are seen in **39N(1)**. Optical micrographs show similar effects to those in the Kevlar rope. There are kink-bands on the inside of a bend in **39N(2)** and also axial splitting due to variable curvature, **39N(3)**. The curve from the straight portion into a kink and then to break at the next kink can be seen in **39N(4),(5)**, and the complications of rupture with fibrillation in **39N(6)**. Two kinks in a fibre in a parallel yarn Twaron rope are seen in **39N(7)** and an anomalous double kink in **39N(8)**. Extensive fibrillation is found in another Twaron rope, **39N(9)**, with detail of peeling in **39N(10)**. An unusual example of damage due to squashing is shown in **39N(11),(12)**.

The pictures in **39O** show that appreciable damage can develop in a thousand cycles of severe tension–tension fatigue in a Dyneema HMPE rope. Indications of axial splitting are seen in **39O(1)**. Kink-bands within fibres, **39O(2)**, develop to project out of the fibre surface, **39O(3)**, and finally into a contorted fibre path, **39O(4)**. These forms are essentially in 'straight' fibre paths. Kinks in whole fibres are seen in **39O(5)–(8)** and accompanied by break in **39O(9)**.

A similar development of kink-bands is seen in a Spectra HMPE rope after a million cycles of less severe tension–tension cycling, **39P(1)–(3)**, with slight fibrillation in **39P(3)**.

Polyester ropes are much less damaged by axial compression fatigue. A million cycles of fairly severe tension–tension cycling leads to the appearance of kink-bands within fibres, **39P(4)**, but these have not developed into cracks that would weaken the fibres. There are some gross kinks, such as **39P(5)**. However, as with the effects of yarn buckling shown in **12M(8),(9)**, the main 'damage' consists of a plethora of transverse lines and some axial cracks, **39P(6)**. Examples of squashing due to lateral pressure are seen in **39P(7),(8)**.

In general, the damage occurring in these ropes, which have been subject to tension-tension cycling is similar to that found from the yarn buckling tests shown in **12L** and **12M**. Axial compression fatigue is a potential hazard in fibre ropes used in deepwater moorings. It can be avoided by maintaining a *high enough minimum* tension on the lines. This is a concept unfamiliar to engineers used to metals, including steel wire ropes, where the concerns are with *maximum* loads, which may cause breakage, and *load ranges*, which lead to metal fatigue.

BEND-OVER-SHEAVE TESTING OF AERIAL CABLES
by Petru Petrina and Leigh Phoenix

At its White Sands Missile Range in New Mexico, the US Army has suspended an aerial cable between two mountain peaks with a span of about 5 kilometers. The cable is equipped with a variable tensioning device to permit moving loads of weights up to 10 tonnes, which may be targets on trolleys for air defence and drop testing, at speeds up to 1000 km/hr. The trolleys are supported on the cable by sheaves (pulleys) and moderate braking forces are applied to stop the trolleys. The cable must have a high strength and low mass per unit length, producing a high transverse wave speed. The jacket must be durable and the cable interior must be tolerant to abrasive actions due to rolling sheaves.

As part of the initial testing which led to the selection of the cable, tests were carried out on readily available, but slightly smaller cables, of similar construction. The basic design was a 36-strand, co-laid aramid Kevlar 29 rope in layers of 6, 12 and 18 strands in a nested helical configuration. The helix angles in all layers was 15°. The inner strands were jacketed in polyester and the outer strands in Kevlar, in order to give greater dimensional stability and resistance to surface wear under the sheaves. This rope had a diameter of 5.3 cm and a break strength of at least 200 tonnes. The actual cable used at White Sands had a diameter of 6.25 cm. The cables were in two forms: unlubricated and lubricated. The former contained the usual fibre finishes, but no additional finishes or lubricants. For the lubricated cable, the Kevlar yarns of the outer braided jacket were impregnated with a blend of silicone and Teflon, which was then cured to a flexible dry state.

The 5.3 cm cables were tested in a cyclic reverse-bend-over-sheave apparatus (CRBOS) in the laboratories of Tension Member Technology, under a cable tension of 50 tonnes and with transverse sheave loads of 2.5 tonnes or less. The sheave to rope diameter ratio was about 6 to 1, giving a short nominal contact length of about 1 cm. Cycle lifetimes ranged from 1300 to 22 000 machine cycles. The upper end of this range was regarded as acceptable for the application. The cable with a lubricated jacket had a much longer life than one that was not lubricated. It was also found that rope lifetime varied inversely approximately with the cube of the sheave load, so that it was advantageous to use more sheaves with lower loads.

Portions of these ropes were dissected and analysed at Cornell University. **39Q(1)** shows a strand where the CRBOS test has worn through the jacket. Within the strands the aramid fibres are fibrillated due to internal abrasion, **39Q(2),(3)**. The wear is greater in the outer strands than in the inner strands. Flattening and fibrillation due to high transverse pressures is also seen, **39Q(4)**. The general conclusion was that damage accumulation was primarily due to local sheave contact and was concentrated most strongly in the outer yarn layers of the outer strands. In unlubricated ropes, fibres were severely crushed and abraded under the jackets, but in the lubricated ropes there appeared to be a cushioning effect. The strength degradation in the fibres of the outer strands was roughly linear with number of cycles. The failure progressed in outer strands by weakening and collapse of the outer layer of yarn, thus overloading inner yarn layers through load transfer until the whole outer strand collapsed.

Unlike typical rope/sheave applications, inter-fibre and inter-yarn abrasion due to relative motion caused by rope bending was not by itself a noticeable cause of abrasive damage under these test conditions.

For further studies on rope wear due to passage over sheaves under tension, a Cornell Cable Wear Testing machine (CCWT) was built and has been reported on by Phoenix *et al* (1993) and Petrina *et al* (1994,1995). These are fundamental studies, but are relevant not only to the White Sands application, but also to plans by the US Navy to replace the 2.5 cm steel wire rope used in the Underway Replenishment System by a fibre rope. In order to simulate the loading of an outer strand in a rope subject to tensile force and lateral loading from a sheave, the strands in the test machine are under tension and experience lateral compression between a Teflon backplate and a rolling sheave. The backplate provides radial constraint to simulate the radial support provided by the inner layer strands to the outer layer strands. The groove of the sheave is about two strands diameter deep and provides lateral constraint to simulate the contact from adjacent strands in the same layer. For a 1 cm strand, the tensile force was about 1.2 tonnes. In order to establish an empirical relation between lateral force and strand lifetime, the lateral sheave load varied with the test from 0.25 to 0.625 tonnes.

In one study, strands were made of 1500 denier Kevlar 29 yarns, with a braided jacket of alternating Kevlar 29 and polyester yarns, which was similar to that used for the outer strands of the White Sands rope. The strands consisted of 3 core yarns, surrounded by a middle layer of 6 yarns and an outer layer of 12 yarns. **39Q(5),(6)** show how fibres can be bent or kinked as a result of the testing. Fibrillation is starting to develop at regions of high strain. Broken fibres, **39Q(7)**, show fibrils which start to coalesce as a result of friction and transverse pressure. This is most severe in the unjacketed strand, when the contact forces cause the fibres to flatten and sinter together forming a structure similar to one obtained by crushing fibres at about the melting temperature. These studies indicate that the forms of failure are influenced by the jacketing. The rolling and sliding of fibres is amplified when no jacket exists and becomes more localized for strands with damaged jackets.

As part of a synthetic fibre rope technology development programme, a series of 1 cm strands with braided polyester jackets was made from different fibres and tested on CCWT. **39R(1)** shows the tendency of Kevlar fibres to split longitudinally and fibrillate as a result of machine cycling. A tensile fracture occurring in such a test, **39R(2)**, also shows a split form, though, as mentioned below, this is not the common form of failure for Kevlar. Splitting and peeling also occur in Vectran fibres, **39R(3)–(5)**, but is less severe than in aramid fibres. Vectran strands lasted over 10 times longer than Kevlar strands. The studies indicated that Vectran and Technora fibres ultimately fail largely in a tensile mode, despite considerable fibrillation due to transverse stresses, whereas Kevlar fibres are more prone to shear failure by splitting along the fibre length producing a wandering crack from one side to the other over many fibre diameters. The Vectran tensile fracture, **39R(6)**, is similar to **39R(2)** for Kevlar.

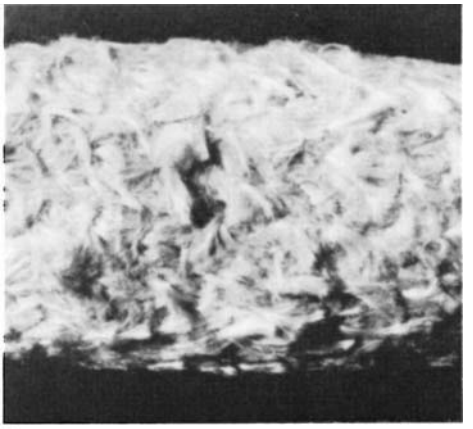

1

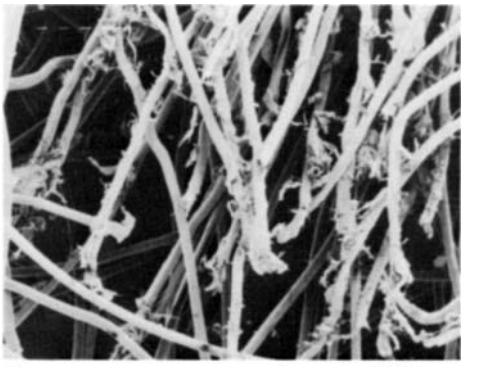

2 200 μm

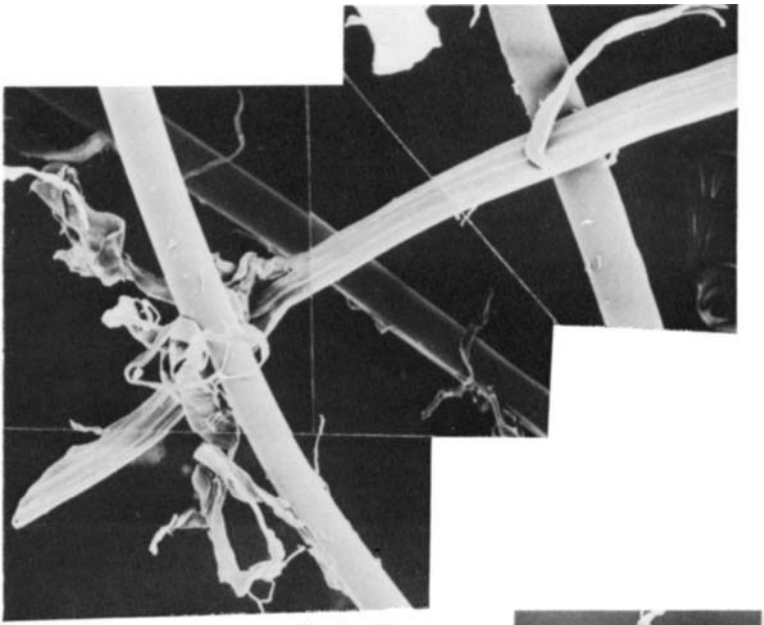

3 20 μm

4 50 μm

5 50 μm

6 50 μm

Plate 39A — Nylon rope cycled wet up to a load of 50% of breaking load, failed after 970 cycles: piece of rope away from break (from OCIMF test).

(1) General view of rope. Note that the rope before testing had a smooth continuous-filament surface, whereas the cycled rope shows many fibre ends sticking out. (2) Broken fibres in inner core region. (3) Detail of fibre splitting and peeling in inner core. (4)–(6) Detail of splitting and peeling in fibres from outer braid.

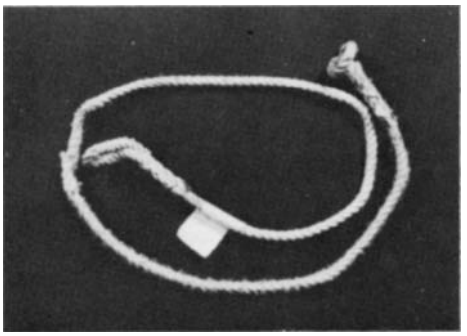

1

2a

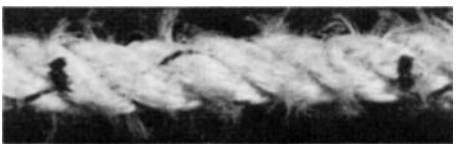

2b

2c

3 — 20 μm

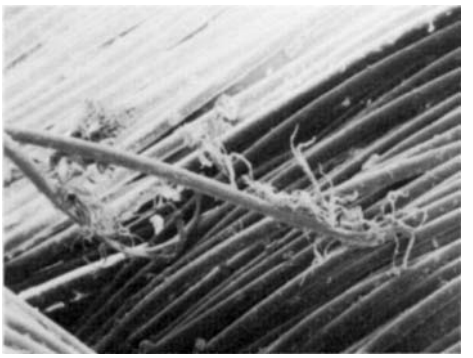

4 — 100 μm

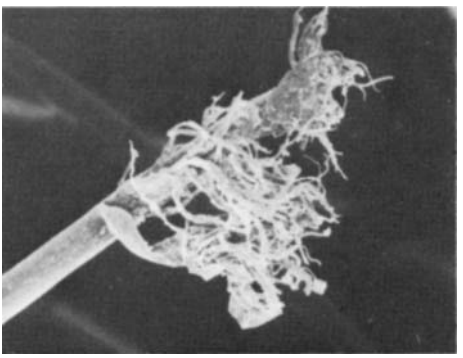

5 — 50 μm

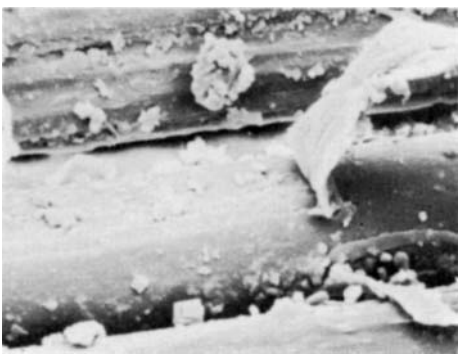

6 — 10 μm

Plate 39B — Nylon rope after use in securing the skirt to the bow of a hovercraft.
(1) The complete rope assembly, which was knotted through an eyelet at the region of severe damage in the middle of the rope on the left. (2) Rope surface in a macrophotograph: (a) region of little damage; (b) region of moderate damage; (c) knot region, with severe damage. (3) Surface of rope in region of little damage. (4) Broken filament in region of little damage. (5) Broken filament in region of moderate damage. (6) Start of fibre peeling in region of moderate damage.

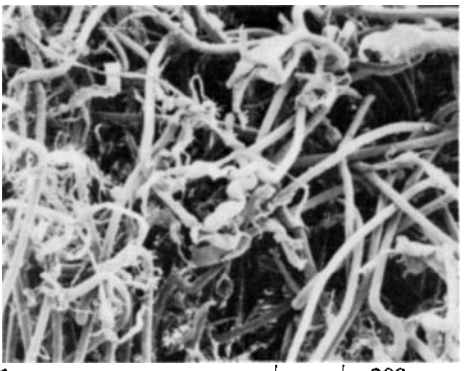

1 200 μm

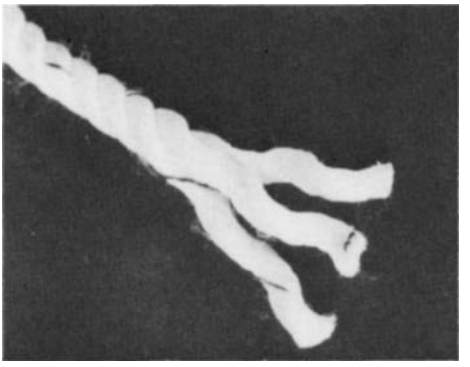

2

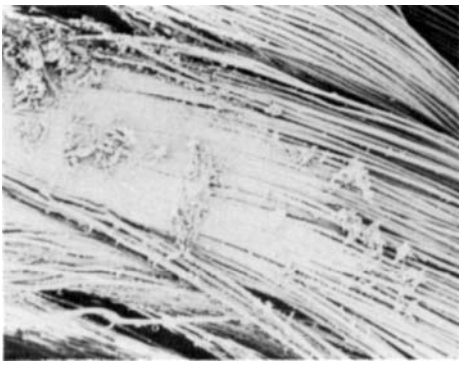

3 500 μm

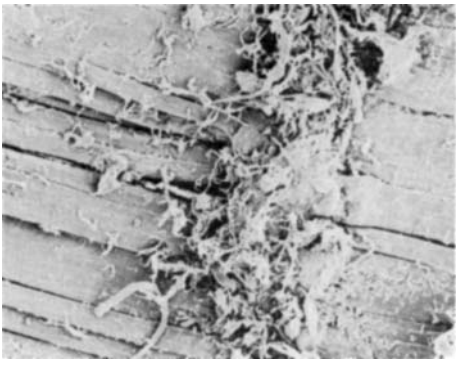

4 100 μm

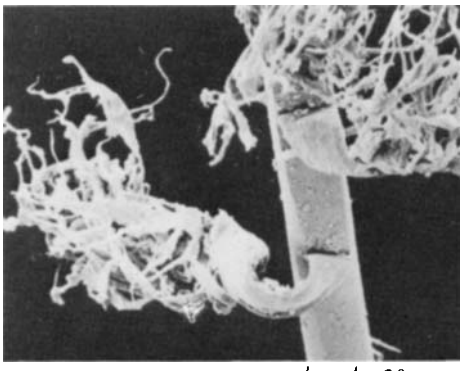

5 20 μm

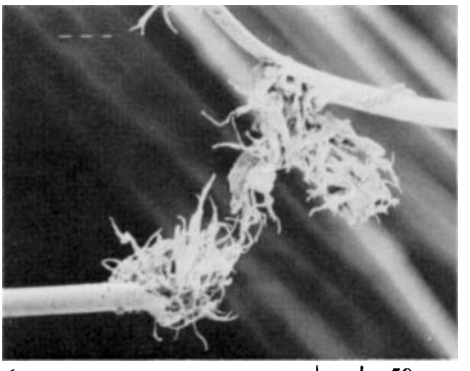

6 50 μm

Plate 39C — Hovercraft rope (continued).
(1) Surface of rope in region of severe damage. (2) Rope in least-damaged region, opened out for examination of inter-strand damage. (3)–(6) Detail of the inter-strand damage in this region.

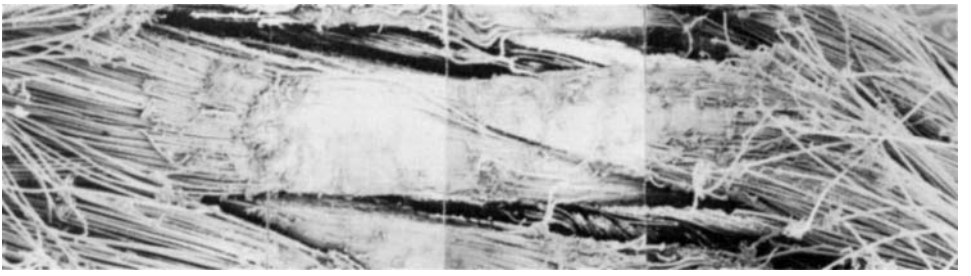

1 ⊢—⊣ 500 μm

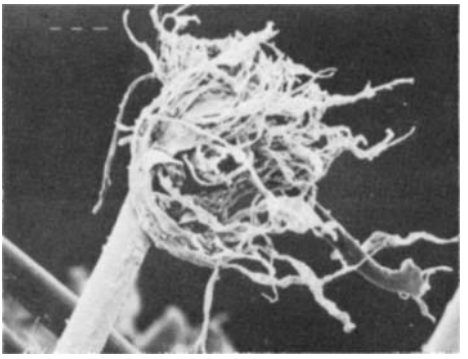

2 ⊢—⊣ 50 μm

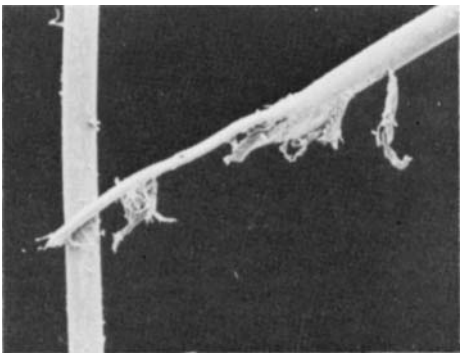

3 ⊢—⊣ 50 μm

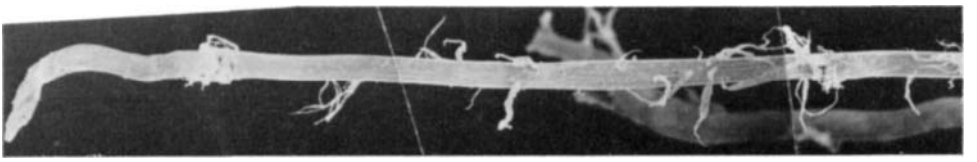

4 ⊢—⊣ 50 μm

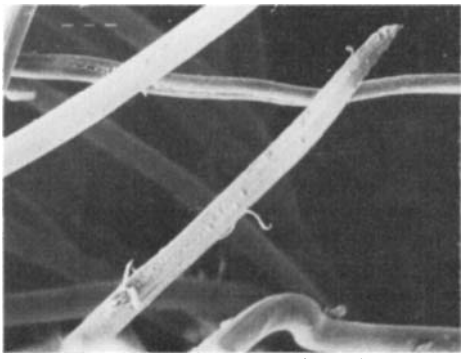

5 ⊢—⊣ 50 μm

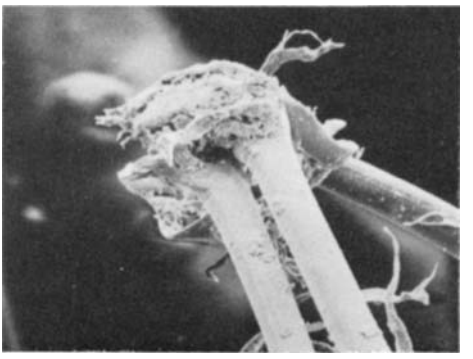

6 ⊢—⊣ 50 μm

Plate 39D — Hovercraft rope (continued).
(1) Inter-strand wear in region of moderate damage. (2),(3) Detail of fibre breakdown in this region. (4)–(6) Fibres from region of severe damage near the knot.

1 100 μm

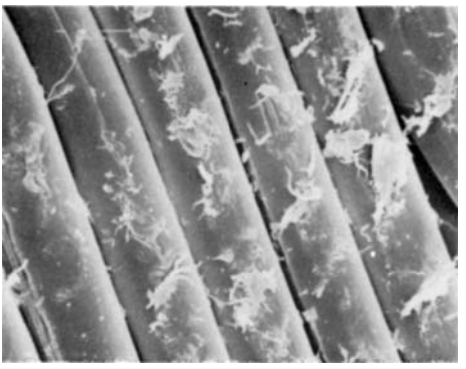

2 20 μm

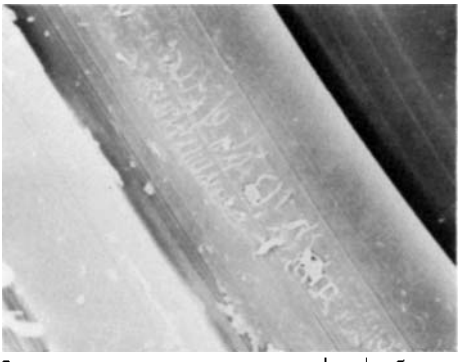

3 5 μm

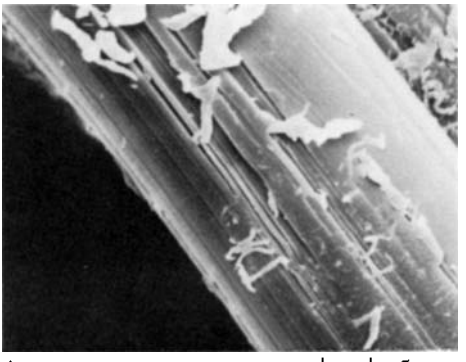

4 5 μm

5 50 μm

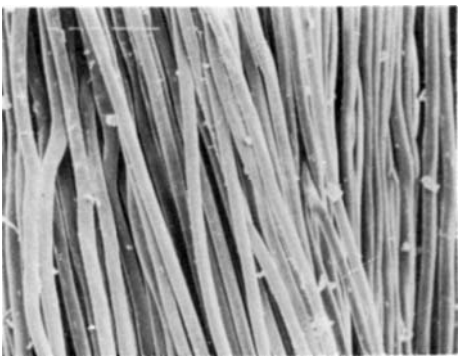

6 100 μm

Plate 39E — Hovercraft rope (continued).
(1) Inner ply yarn from least-damaged region. (2)–(4) Detail of fibre damage in this yarn. (5) Outer ply yarn from least-damaged region. (6) Inner ply yarn in a region of more severe damage.

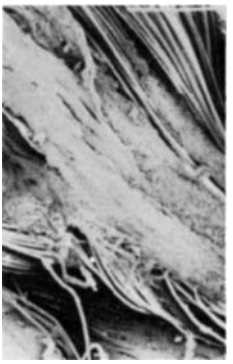

1a ⊢—⊣ 1 mm

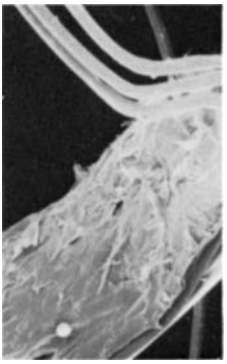

1b ⊢—⊣ 100 μm

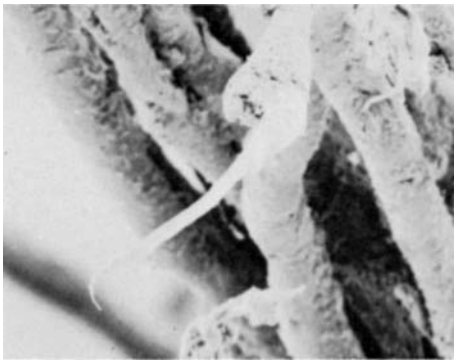

2 ⊢—⊣ 50 μm

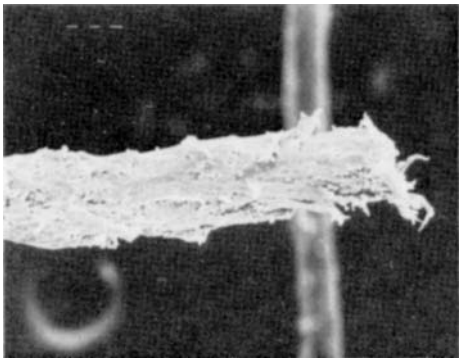

3 ⊢—⊣ 50 μm

4 ⊢—⊣ 20 μm

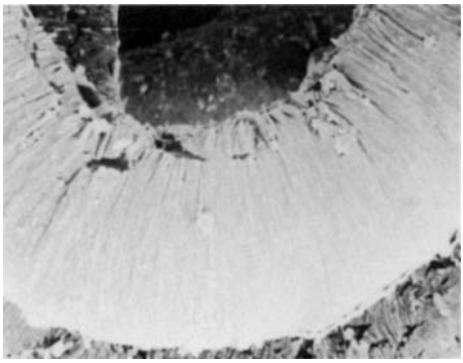

5 ⊢—⊣ 10 μm

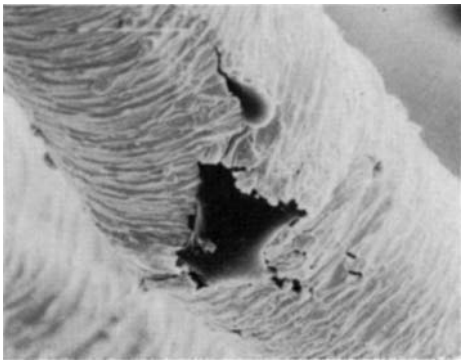

6 ⊢—⊣ 5 μm

Plate 39F — Broken kinetic energy recovery rope (KERR).
(1) Strands away from break in two ropes. (2), (3) Fibre breaks in first rope. (4), (5) Fibre surface changes in first rope. (6) Fibre from second rope.

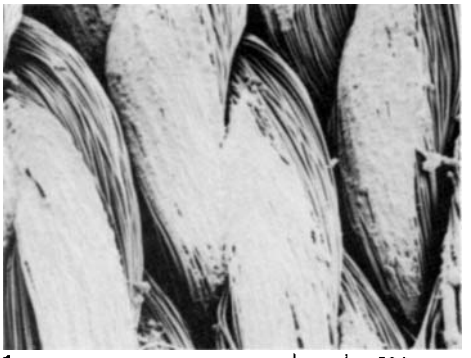

1 ⊢—⊣ 500 μm

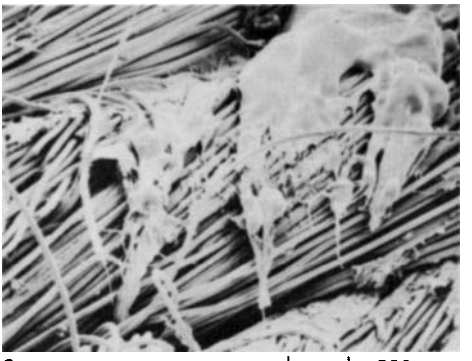

2 ⊢—⊣ 200 μm

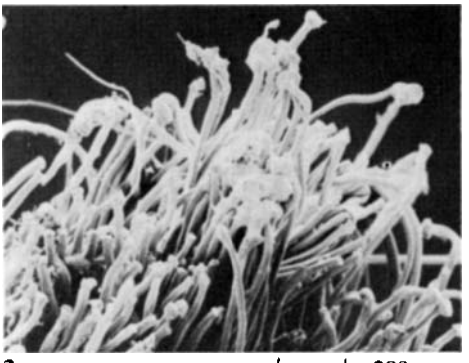

3 ⊢—⊣ 200 μm

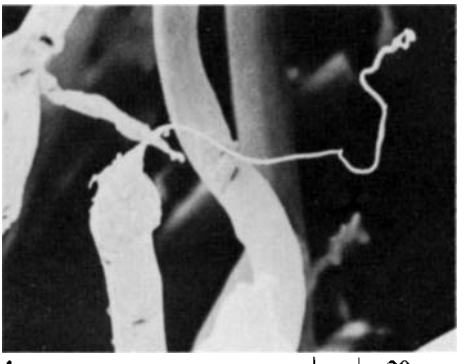

4 ⊢—⊣ 20 μm

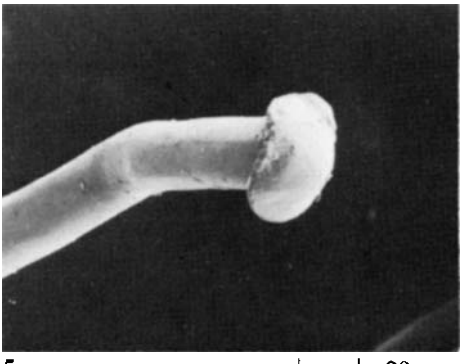

5 ⊢—⊣ 20 μm

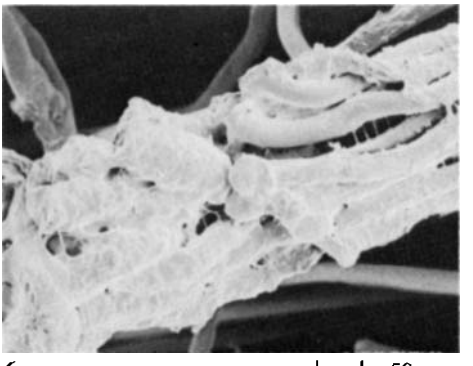

6 ⊢—⊣ 50 μm

Plate 39G — Polyester rope heated to 160°C for 33 hours and then broken in a tensile test.
(1) Surface of unbroken strand in rope broken at room temperature. (2) Surface of broken strand in rope broken at room temperature. (3) Broken inner yarn from rope broken at room temperature. (4) Fibre end from this broken yarn. (5) Fibre end from broken yarn in rope broken hot. (6) From broken outer yarn in rope broken at room temperature.

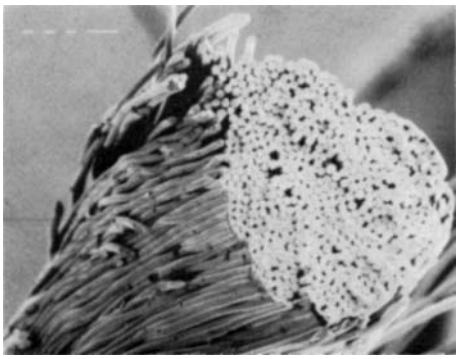

1 200 μm

2 50 μm

3 10 μm

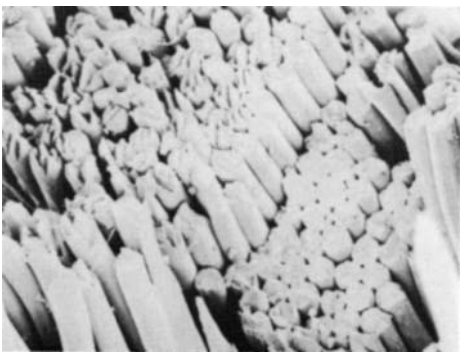

4 50 μm

5 5 μm

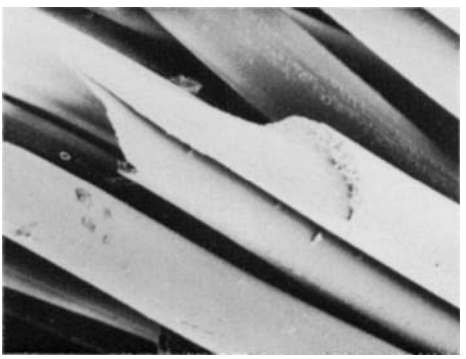

6 20 μm

Plate 39H — Nylon 6 rope heated to 160°C for 33 hours and then broken in a tensile test.
(1)–(3) Yarn from rope broken hot. (4),(5) Inner yarn from rope broken at room temperature. (6) Filament from outer yarn in rope broken at room temperature.

1 50 μm

2 10 μm

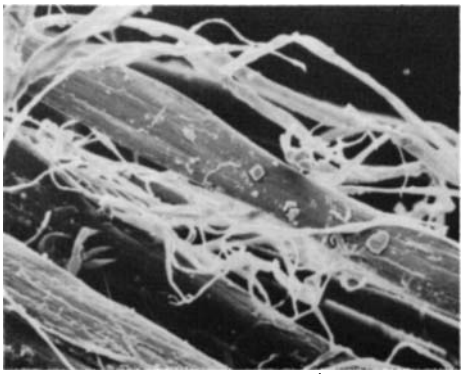

3 10 μm

4 50 μm

5 200 μm

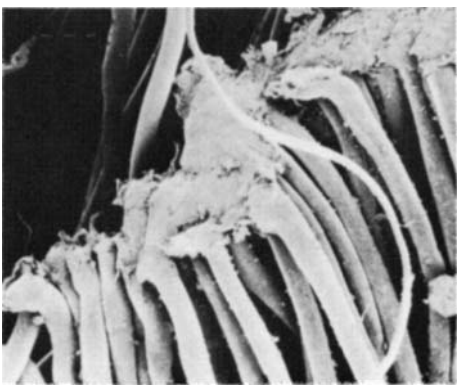

6 20 μm

Plate 391 — Kevlar rope used for Genoa sheet.
(1) Fibre breakdown by fibrillation. (2),(3) Detail of damage, showing presence of salt crystals.
Used ropes from RAE.
(4) Nylon mountain rescue rope. (5) Polypropylene glider tow rope. (6) Aircraft barrier rope.

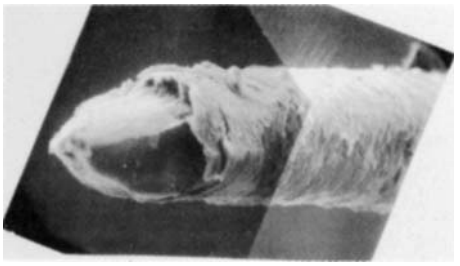

1

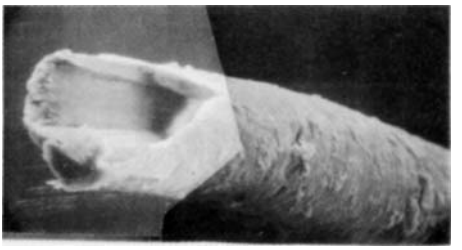

2

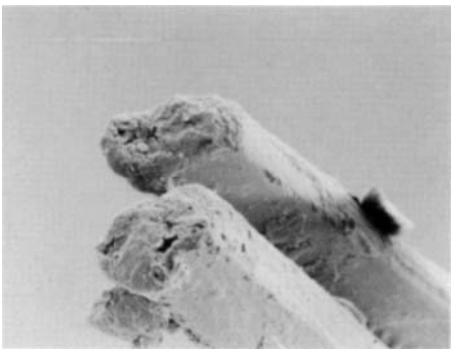

3

4

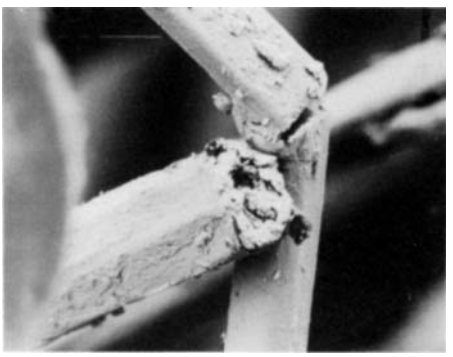

5

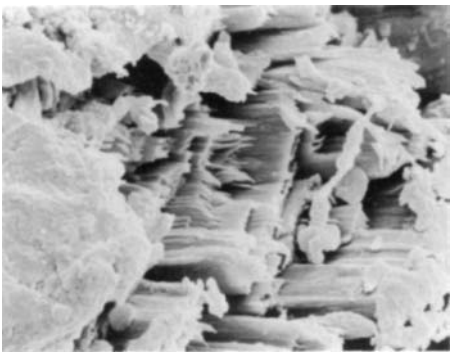

6

Plate 39J — Damage in a nylon mooring line, by courtesy of S. Backer, MIT.
(1),(2) Opposite ends of a broken filament from a 3-strand nylon rope after several years of use.
Laboratory break test at RAE of unused flax rope.
(3),(4) Flax fibre rupture. (5) Kink-band failure, possibly on snap-back. (6) Detail of internal rupture of flax fibre.

1

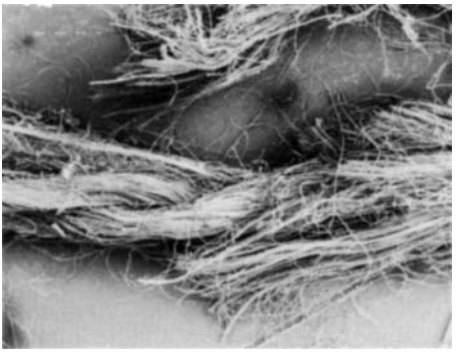

2

3

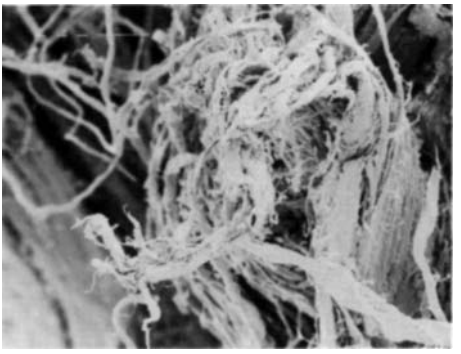

4

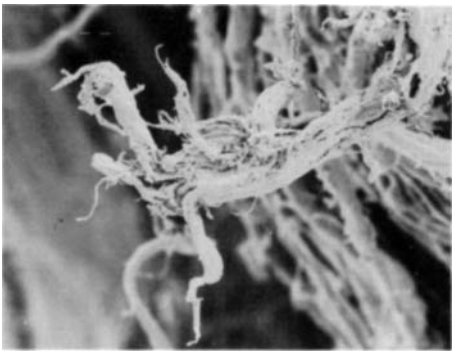

5

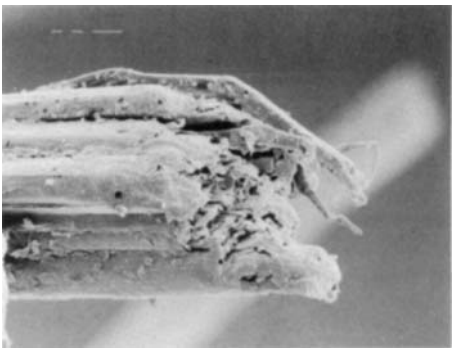

6

Plate 39K — A worn flax rope from RAE.
(1) External abrasion. (2) Separate strand breaks. (3) Disturbance at strand break. (4)–(6) Fibre breaks.

1

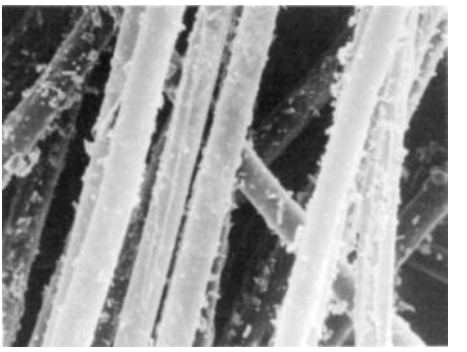

2

3

4

5

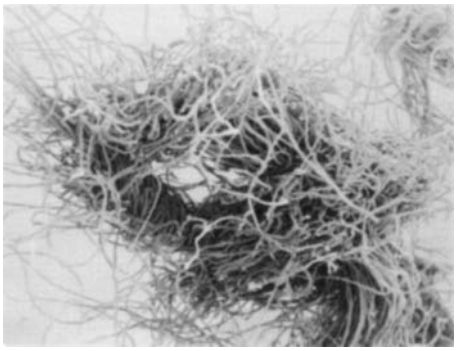

6

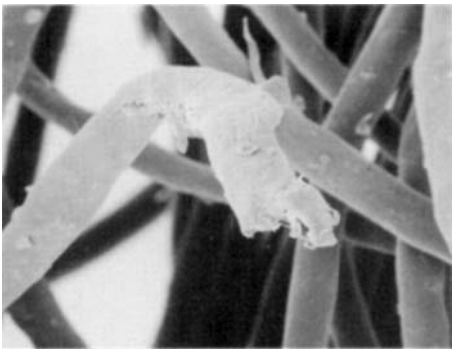

7

Plate 39L — A polyester multi-strand rope after use in a trial mooring for two years.
(1) Mating point between strands within rope with little damage. (2) Slight peeling and accumulation of debris. (3)–(5) Broken fibre ends. (6) Damaged region of rope jacket. (7) Broken fibre from jacket.

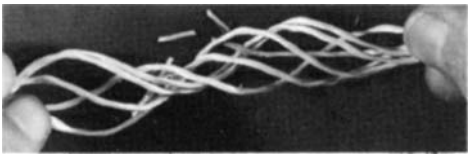

1

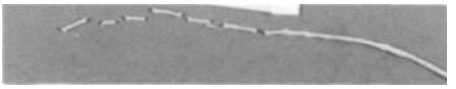

2

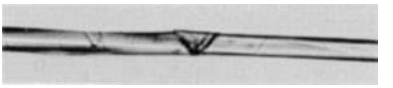

3

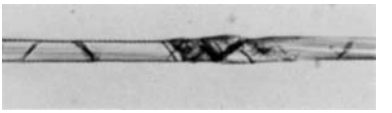

4

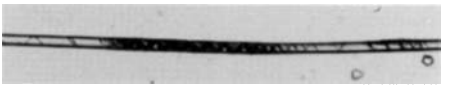

5

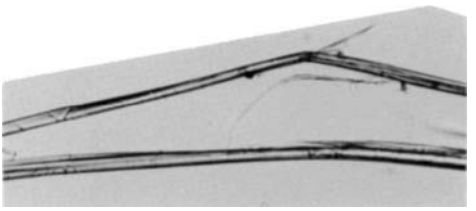

6

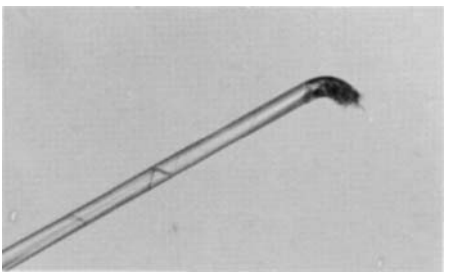

7

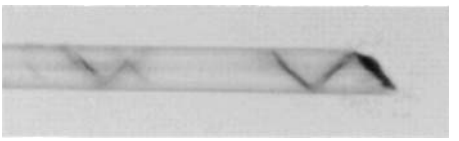

8

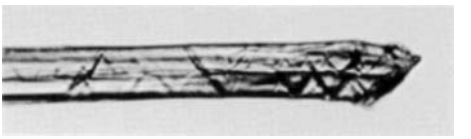

9

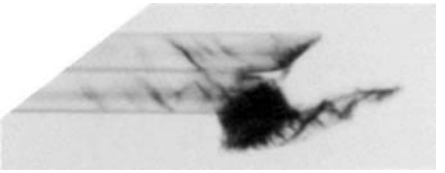

10

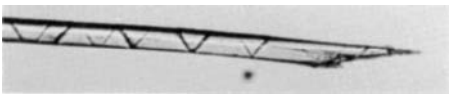

11

12

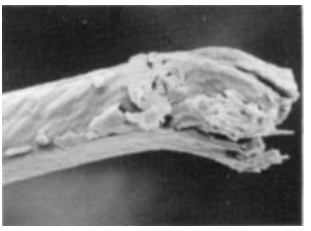

13

14

15

Plate 39M — Five tonne aramid Kevlar 129 rope in a 6-round-1 twisted wire-rope construction after 1 000 000 cycles tension–tension fatigue between about 10 and 50% of break load (60 kN), centre yarn of core strand.

(1),(2) Broken into pieces between 2.5 and 5 mm long. (3)–(5) Kink-bands within fibres. (6) Kink of whole fibre. (7) Break at kink in fibre. (8)–(15) Fibre breaks, along kink-bands and with axial splitting.

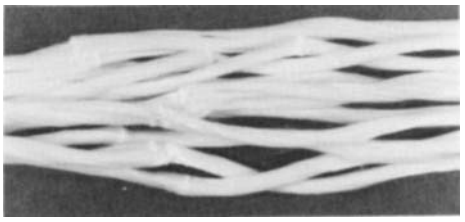

1

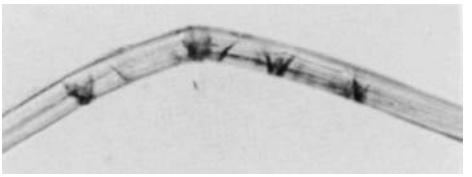

2

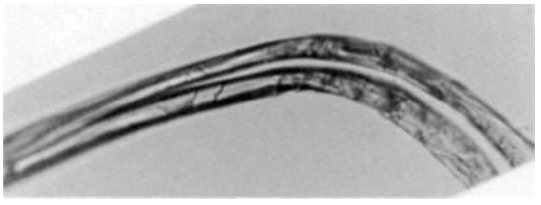

3

4

5

6

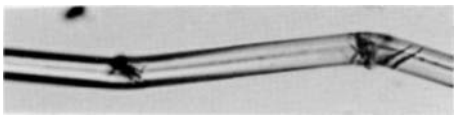

7

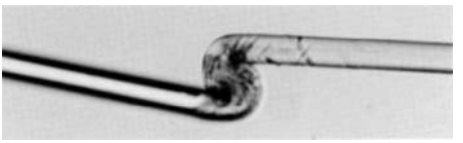

8

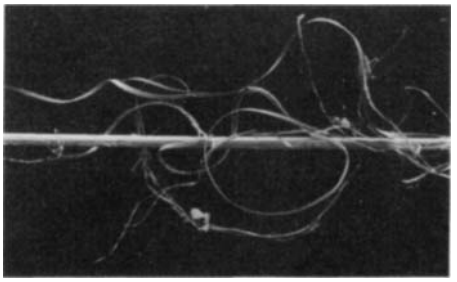

9

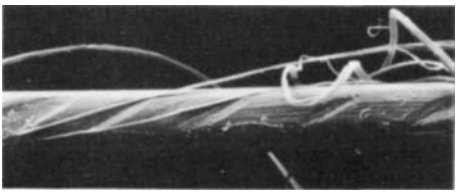

10

11

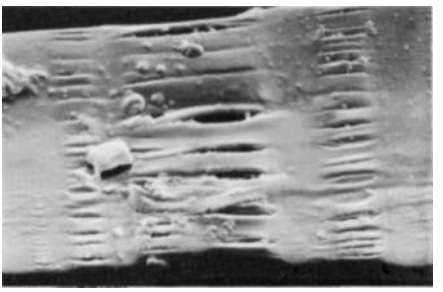

12

Plate 39N — Five tonne aramid Twaron 1000 ropes, after 1000000 or more cycles of tension–tension cycling between about 20 and 60% of break load.

(1) Kinks in yarns at interval along a yarn. (2) Kink-bands in a fibre. (3) Axial split. (4),(5) Bending into a kink and then to a break. (6) Break with fibrillation. (7) Two kinks. (8) Double kink. (9),(10) Fibrillation and peeling from fibre surface. (11),(12) Squashing of fibre.

Note: (1),(9)–(12) Simulated 36-strand torque-balanced rope. (2)–(6) 6-round-1 wire rope construction. (7),(8) Parallel yarn rope.


1


2


3


4


5

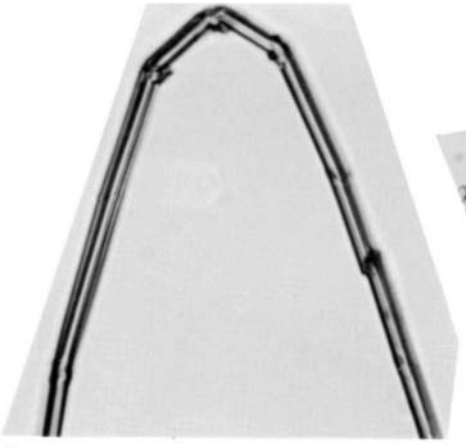
6

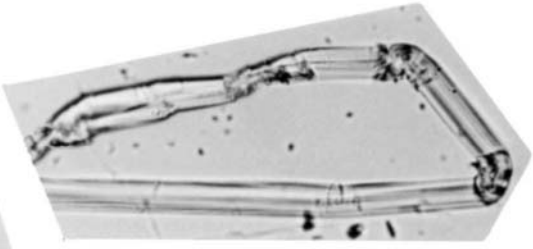
7

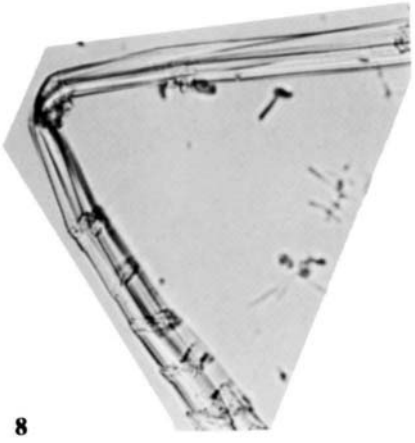
8

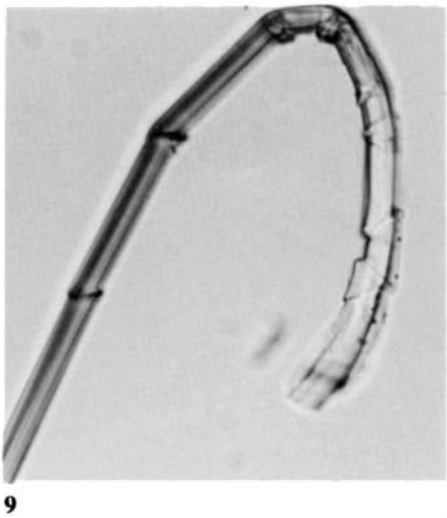
9

Plate 39O — Five tonne HMPE Dyneema SK60 6-round-1 wire-rope construction after 1080 cycles of tension–tension fatigue between about 10 and 70% of break load had led to failure at the termination. (1) Indications of axial splitting. (2)–(4) Localised kink-bands in the fibre of increasing severity. (5)–(8) Severe kinks in the whole fibre. (9) Kink and break.

1

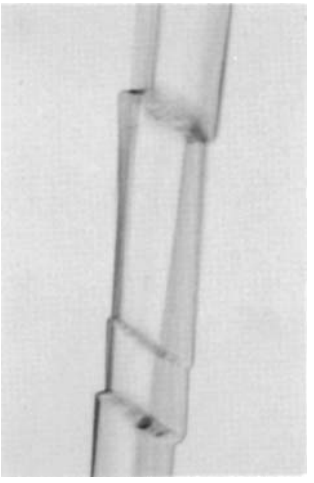

2

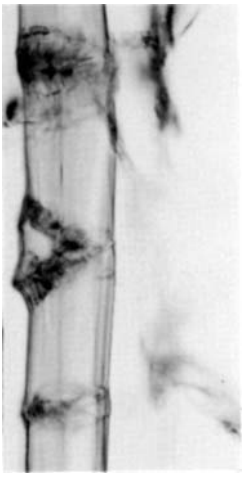

3

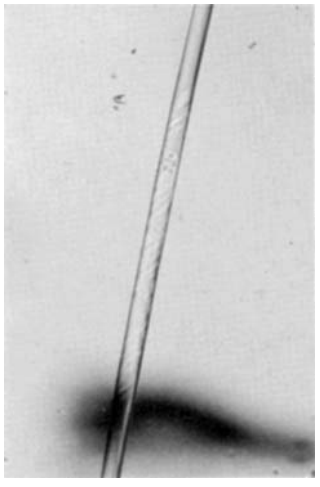

4

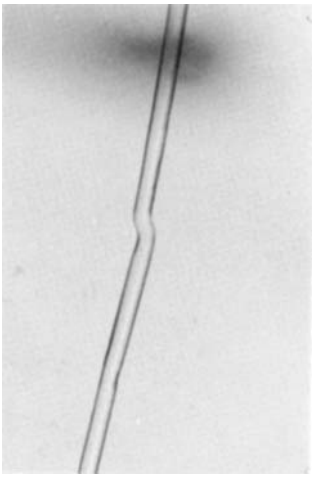

5

6

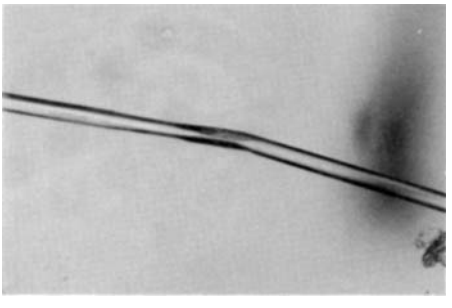

7

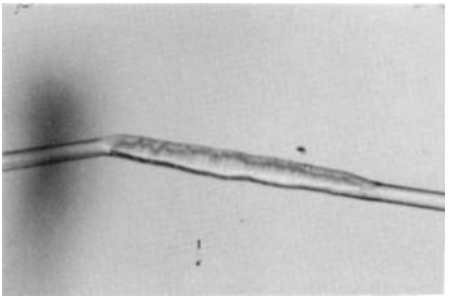

8

Plate 39P — Five tonne HMPE Spectra 900 6-round-1 wire-rope construction after 1000000 cycles of tension-tension fatigue between about 25 and 55% of break load.

(1)–(3) Kink-bands and slight fibrillation.

Five tonne polyester 6-round-1 wire-rope construction after 1000000 cycles of tension–tension fatigue between 17.7 and 62.5% of break load.

(4) Faint internal kink-bands. (5) A gross kink in a fibre. (6) Transverse lines and axial cracks. (7),(8) Squashing due to lateral pressure between fibres.

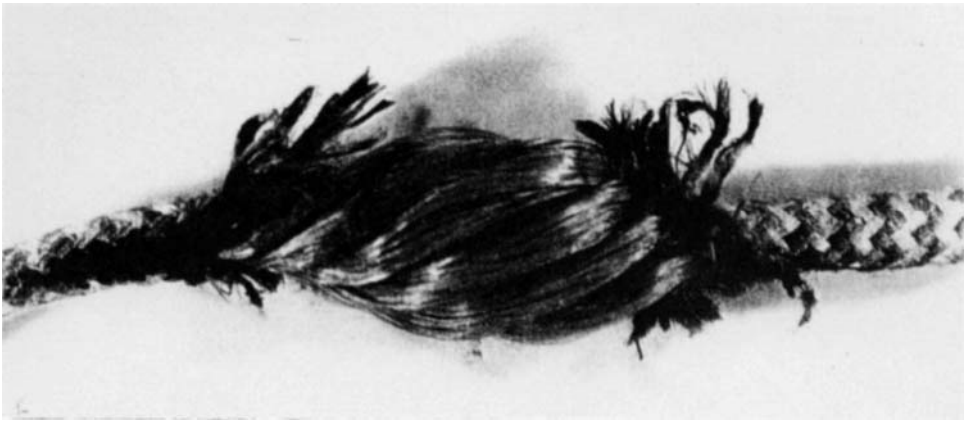

1

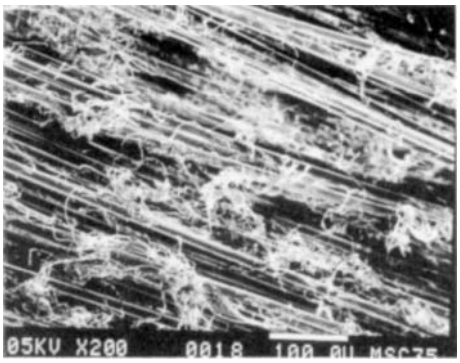

2

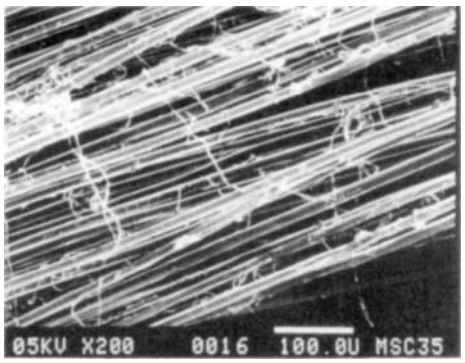

3

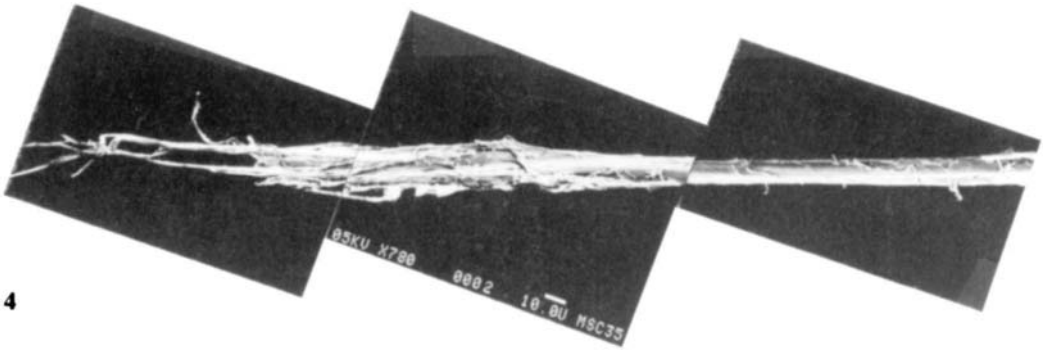

4

5

6

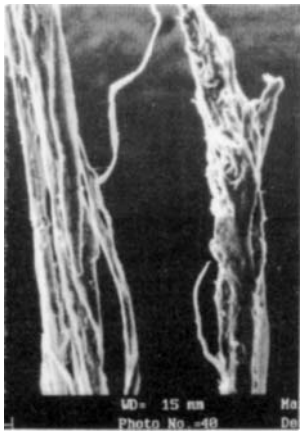

7

Plate 39Q — Cyclic reverse-bend-over-sheave testing of 2.5cm diameter Kevlar aramid rope.
(1) A strand with broken jacket. (2) Fibres from an outer layer strand. (3) Fibres from an inner layer strand. (4) Flattening and fibrillation due to excessive transverse pressure.
Kevlar strand tests on the Cornell cable wear tester.
(5) From half-jacketed strand tested to failure at 225kg. (6) From a fully jacketed strand failed at 320kg. (7) From an unjacketed strand failed at 320kg.

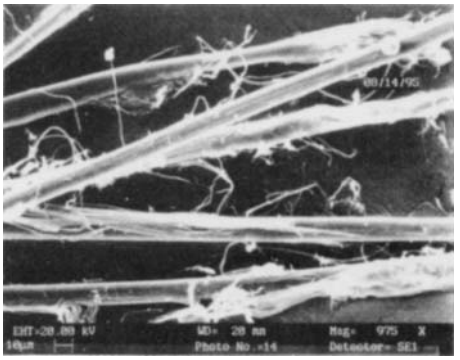

1

2

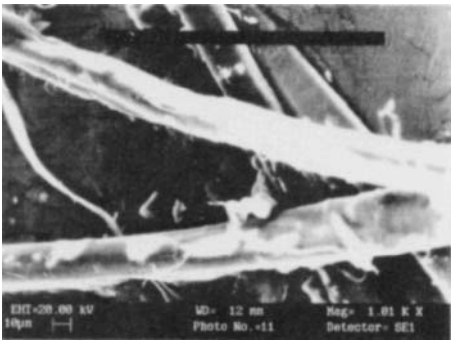

3

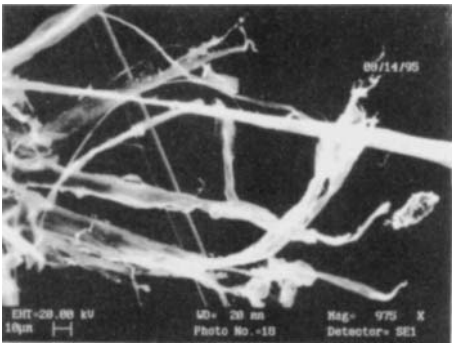

4

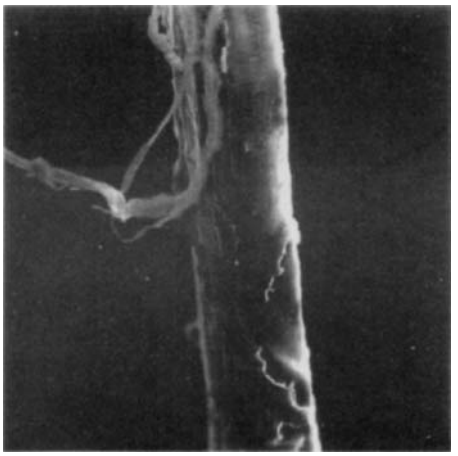

5

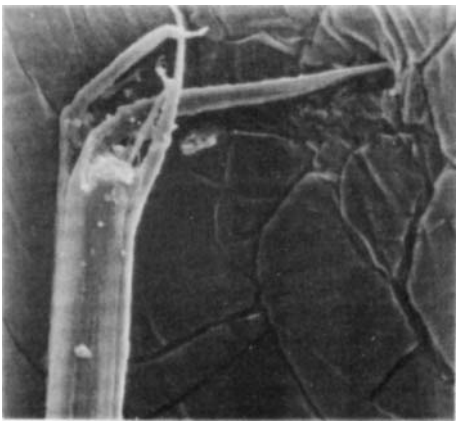

6

Plate 39R — Strand tests on the Cornell cable wear tester.
(1),(2) From Kevlar strands. (3)–(6) From Vectran strands.

40

OTHER INDUSTRIAL PRODUCTS

This last chapter on industrial uses contains a miscellany of products used for a variety of purposes.

The first example is a faded orange-coloured coated fabric from a wind-cone (wind-sock), which had been taken out of service after the usual period of about six months use on an airfield to show wind direction. In manufacture, the nylon 66 base fabric had been primed with isocyanate and then coated with a thin layer of white Hypalon (chloro-sulphurated polyethylene) followed by a thicker coating on the outside of fluorescent orange Hypalon.

The exposure to the mechanical action of wind forces and to ultraviolet radiation and other environmental effects had caused the coating to break along lines both along and across both faces of the sample. The nylon fabric was visible under the cracks, some of which were straight and followed the line of warp or weft yarns. Other cracks meandered irregularly across the fabric, but curved roughly in a direction which was presumably a result of the particular usage. The coating at the edge of the cracks was loose and easily removed. The most severe damage was a slit, 9.5 cm long, where all the warp yarns had broken, together with two or three weft yarns. In other bare areas there was partial breakage, with some warp yarns but no weft yarns severed.

In relatively undamaged material, shown in cross-section in **40A(1)**, there is good contact between the nylon yarn and the plastic coating; but the first sign of damage is a separation of coating from the yarn crowns, **40A(2)**. The separations can join up to give long lengths of coating which are no longer bonded to the nylon, although this may not be apparent on superficial examination of the material. Once the coating is loose, it is no longer supported by the strong nylon yarns, and it begins to break up and lift off the surface, **40A(3)**. If the fabric specimen is bent into a V along a line of wear, the depth of separation of coating from the fabric is clearly shown, **40A(4)**.

Examination of the face of the coated fabric reveals a pattern of small cracks in the thick Hypalon layer as the first indication of breakdown, with the nylon fabric (highlighted by charging in the electron beam) beginning to show through, **40A(5)**. On the reverse side, with a thin Hypalon layer, the damage was much more severe, **40A(6)**.

Along worn lines, where the exposed underlying fabric had not broken completely, some filament breaks can be seen, **40B(1)**, together with long splits penetrating down into the filaments, **40B(2)**. Surface peeling of filaments can also be seen, **40B(3)**.

Complete breakage of yarns is shown in **40B(4a)**, and often runs straight across a line of yarns, **40B(4b)**. Damage to the filaments can be detected some way back from the broken end, **40B(5)**, and is characterized by splitting. A long central split at the end of a broken filament can be seen in **40B(6)**, although the ends become rounded by further wear. This form of filament failure probably results from repeated bending, as shown in laboratory flex fatigue (Chapter 12).

The major cause of damage of the material is wind flagellation, possibly accelerated by other environmental degradation. The complex rippling motion, due to wind forces, first causes the coating to separate from the fabric. It is only after this has occurred that the fabric begins to be damaged, because bending becomes concentrated where there are cracks in the coating. Ultimately this leads to the breakage of fibres by flex fatigue.

The effect of natural weathering can be seen in a polyester fabric, which had been used in the form of two burgees flying at the mast-head of sailing dinghies for two or three seasons. The first burgee had almost disintegrated, and was torn at the edges, **40C(1)**. The filament break, **40C(2)**, is typical of light-degraded material. Away from the breaks the fibre surfaces have a rough and pitted appearance, **40C(3)**, and loss of material, **40C(4)**. At high magnification it can be seen that, in addition to the holes, there are many fine cracks or crazes

perpendicular to the fibre axis, **40C(5)**. The other burgee was not quite as badly damaged, and it shows holes, but no fine crazes, on the fibre surfaces, **40C(6)**. The general impression is of weakening of the fibre due to the influence of light and perhaps some chemical action, with a few broken filaments on the yarn crowns, but most of the filament breakage concentrated in the tears along both warp and weft directions.

The next four examples are from sporting uses. The breakage of the shaft of a carbon fibre/epoxy badminton racket illustrates in real use the type of failure found in composite testing, as illustrated in Chapter 26. The shaft had broken near the point at which it joined the head of the racket. A general view of the fractured end is shown in the photograph, **40D(1)**. The shaft, which is made by winding angled plies of carbon fibre, is hollow; but some glue filling the central hole can be seen in the SEM view, **40D(2)**. The breakage of the several layers of carbon yarns is clearly apparent in **40D(2),(3)**. The effects observed and shown in **40D(4)** include fibre breakage, fibre pull-out and delamination. The detail of individual fibre breaks can be seen in **40D(5)**, and of delamination in **40D(6)**.

The second example is a string from a badminton racket, **40E(1)**, which has broken where strings cross, **40E(2)**. At the centre of the racket there is general wear, shown by peeling away of fibrils from the surface of the string, **40E(3)**. The actual break, which is a single sudden event, shows a complicated morphology, **40E(4)–(6)**.

The break of a tennis racket string (Donnay GLM 640) is shown in **40F(1)**. Near the break a line of cracks can be seen on the outer sheath, **40F(2)**. The fibre breaks, **40F(3),(4)**, appear to consist of some cutting of ends or damage by high localized pressures and some bulbous high-speed breaks, which probably occur during final failure of the string after it has been previously weakened by the other forms of damage.

The third sporting example is a bowstring used in archery, in which one strand had broken, **40F(5),(6)**. There is considerable peeling of filaments, which presumably caused weakness, and the broken ends are then high-speed breaks, with some pulling out of molten tails.

The photographs in **40G** and **40H** illustrate some other forms of damage to fibres. The first, **40G(1),(2)**, is a thick nylon 6 monofil used to transport sheets through an automatic laundry. The form of damage is extensive peeling of the monofilament surface, which was very severe even after only 10 hours service. Nylon 610 performed better, and showed a similar level of damage after 50 hours, and nylon 11 was very much better, with only a small amount of peeling after 257 hours service.

Another type of break is shown in **40G(3)**. This is a very clear example of failure by the kinkband mode, discussed in Chapter 12. It is an optical micrograph by the late S. C. Simmens of the Shirley Institute of nylon filaments from the inner layers of a tyre, which had been worn by simulated use on a rotating drum in a test bed. The damage may be due to compression on the inside of a bend, but could be due to compression of the whole fibre within the rubber matrix. It is true to say that this fibre failed by breakage at a kinkband under compression; but this is not necessarily, or even probably, the cause of failure of the tyre. The real cause may have been a loss of adhesion between the nylon and the rubber, which then allowed the fibre to suffer the deformation leading to its rupture.

A break which appears to be a tensile fatigue break of nylon, as described in Chapter 11, is shown in **40G(4)**. The characteristic tail of the fatigue break can be seen. This break was a fibre from a cord of a parachute, which had been deployed to assist braking of fighter aircraft on landing. The parachute flutters at about 50 Hz and each deployment lasts about 2 minutes, so that the fibres would experience over 100 000 cycles of tensile stress in 20 deployments. The tensile fatigue mechanism is thus a likely cause of damage to the fibre, provided the stress on a fibre falls to zero in each cycle. This is possible since there may well be an alternation of tension and compression waves.

An industrial example of the cutting of filaments is shown in **40G(5)**. This is a small hole in a polypropylene fabric, which is used to filter china clay. The filaments are sheared off at an angle, **40G(6)**, and the breaks were probably caused by a small hard object being forced through the fabric.

The effects of severe light degradation in polypropylene are illustrated in **40H(1)**, in a study reported by Barish (1989). The filaments are from the top of the back cushion of a car seat, where the material had been exposed to light but not to much mechanical wear for about five years. It is known that polypropylene shrinks under these conditions, and, after straightening out crimp, would generate tension. In the weak degraded material on the filament surface, the tensile stress is relieved by the formation of transverse cracks. The boundary between degraded and regular material can be clearly seen in a fibre which has been split open, **40H(2)**.

We next turn from heavy industrial use to personal hygiene. In an unused toothbrush the bristle has an end with a shape determined by the cutting, **40H(3)**; but, after use, this has become somewhat rounded, **40H(4)**, and the surface of the bristle is beginning to wear by surface peeling.

The etfects of high-speed ballistic impact are shown in studies by C. Cork at UMIST. A bullet fired at 514 m/s at a nylon fabric penetrates the material and breaks the nylon fibres, **40H(5)**, with the typical high-speed rupture form, shown in Chapter 6. Nowadays, Kevlar has replaced nylon as the material used in 'bullet-proof vests'. Under ballistic impact it fails by axial splitting, **40H(6a,b)**, in a manner similar to a slow-speed tensile break.

An example of failure caused by direct surface wear is shown in **40I**. This is a shoe-lace,

which had broken after comparatively little use, as a result of rubbing against the metal eyelets. The outer cover of the lace is a viscose rayon braid, **40I(1)**, in which the fibre surfaces had been worn flat, **40I(2)**, and then had eventually broken. The broken ends can be seen in the interstices of the braid, **40I(3a,b)**. An unusual broken rayon fibre, from close to the place where the braid had broken, is shown in **40I(4)**. The exposed cotton yarns of the core, **40I(5)**, had then broken by multiple splitting, **40I(6)**. A higher-quality lace would be of stronger fibres, such as nylon.

Papermakers' felts are subject to severe forces in hot wet conditions as they are driven through the machines and compressed between rollers. M. A. Wilding and C. Cork at UMIST have examined the damage which can be seen in used felts. Only limited details of the construction and use of the felts, which are made of nylon fibres, were available. **40J(1)** shows the surface of an unused felt, including a bulbous end, probably resulting from some heat treatment. Bulbous ends are most common on the paper side. Cut ends are also found. After use, **40J(2)**, there is considerable surface wear of the fibres, flattening and multiple split breaks. These effects are also seen in part-used felts. The felt in **40J(3)** contains a mixture of coarse (44 dtex) and finer (17 dtex) fibres and shows severe wear after 2 days use, with considerable splitting and peeling of fibres. The damage appears to be less severe after 14 and 16 days respectively in **40J(4),(5)**, which are made of finer fibres (3.3 and 6.7 dtex, respectively), though there is considerable flattening and some splitting. **40J(6)** shows clear examples of multiple splitting failures.

Filter fabrics can suffer damage from chemical and thermal attack as well as mechanical action. The pictures in **40K** are of a degraded polypropylene filter after use at 110°C. The yarn break in **40K(1)** can be seen in **40K(2)** to include a mixture of stake-and-socket breaks, which, as shown in **16D(1)**, are common after chemical attack, and axial splitting. In other places, **40K(3)**, the fibres break into short pieces. Earlier stages of the thermal and chemical attack are shown in **40K(4)–(6)**. Extensive transverse cracking leads to portions of material breaking away.

The rupture of nylon and Kevlar fibres as a result of ballistic impact are shown in **40H(5),(6)**, but in view of the limited information on the form of damage by bullets, as referred to in Chapters 44 and 46, it is worth including more pictures from the laboratory studies of C. Cork at UMIST. When a bullet impacts at high speed on a woven fabric, a pyramidal out-of-plane wave propagates across the specimen, **40L(1)**, preceded by an in-plane wave, which contributes to the increase in length. In a more isotropic knit fabric, **40L(2)**, the deformation is conical. After a nylon fabric has been penetrated at the comparatively slow speed of 254 m/s, **40L(3)**, there is extensive local damage around the hole made by the bullet and the effects of the in-plane extension along the warp and weft directions can be seen reaching to the edge of the fabric specimen. At the higher speed of 514 m/s, **40L(4)**, the hole is much sharper and the warp and weft deformation lines do not extend as far, because penetration has been completed before the wave reaches the edge of the circle. Similar differences are seen in a Kevlar fabric, **40L(5),(6)**.

1 100 μm

2 100 μm

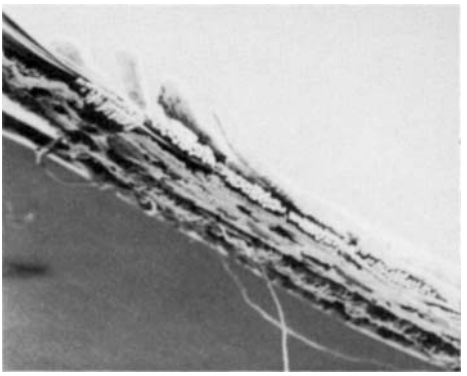

3 500 μm

4 500 μm

5 1 mm

6 1 mm

Plate 40A — Examination of worn wind-cone.
(1) Cross-section of relatively undamaged material. (2) Cross-section showing initial indication of damage. (3) First signs of break-up of coating. (4) Specimen folded into a V-bend, showing large areas of loss of bonding between fabric and coating. (5) First signs of damage on the face of the material. (6) More severe damage on the reverse side.

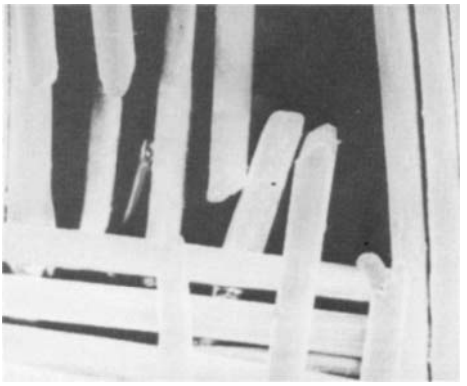

1 500 μm

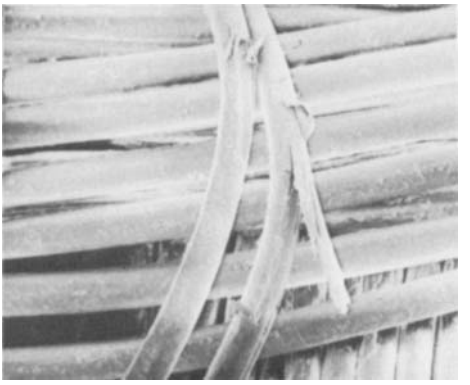

2 500 μm

3 500 μm

4a 1 mm

4b 1 mm

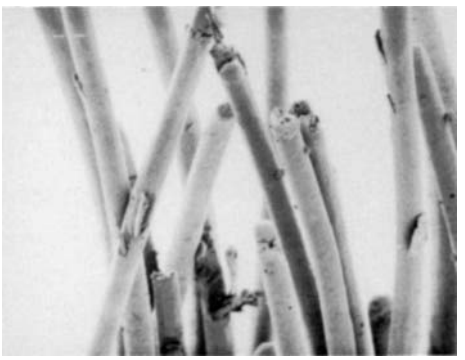

5 500 μm

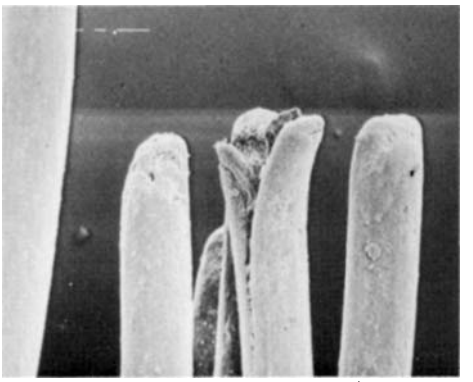

6 20 μm

Plate 40B — Examination of wind-cone (continued).
(1) From region where fabric is exposed, but yarns are not broken, except for a few filaments. (2),(3) Development of filament damage. (4a, b) Regions of more severe wear. (5) Filaments some distance back from a yarn break. (6) Filaments at a yarn break.

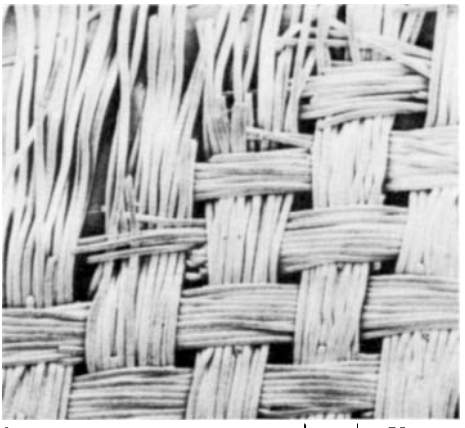

1 50 μm

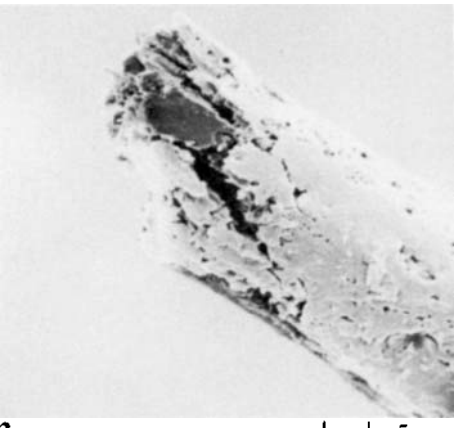

2 5 μm

3 10 μm

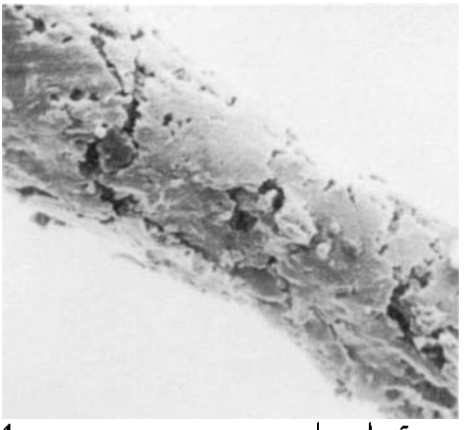

4 5 μm

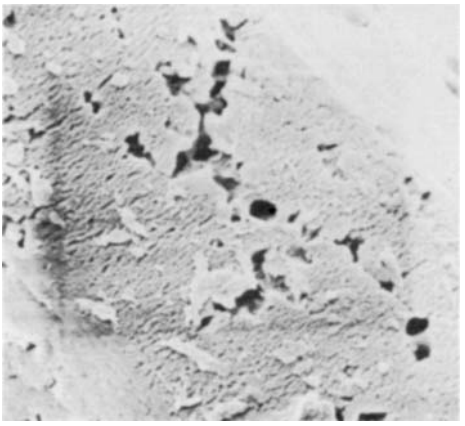

5 2 μm

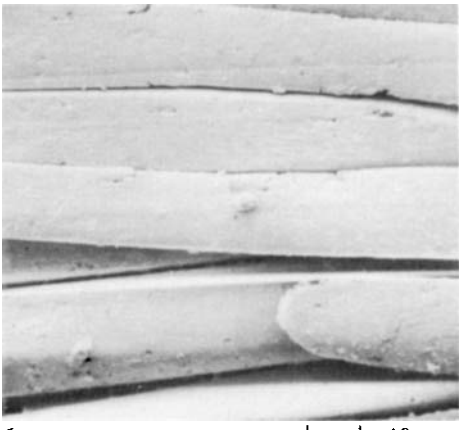

6 10 μm

Plate 40C — Natural weathering of burgees on a sailing dinghy.
(1) Torn region at edge of fabric. (2) Broken end of filament. (3) Surface of yarn crowns, with one broken filament. (4) Part of fibre away from broken end, with thinning due to loss of material. (5) Crazing of filament surface. (6) Second burgee, not as severely damaged.

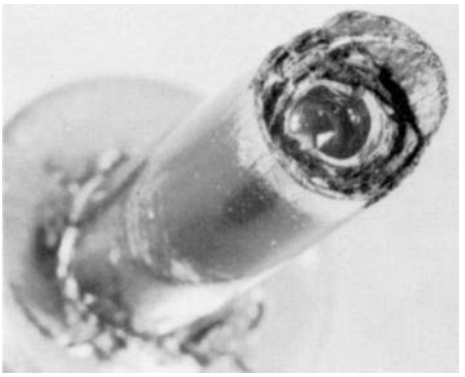

1

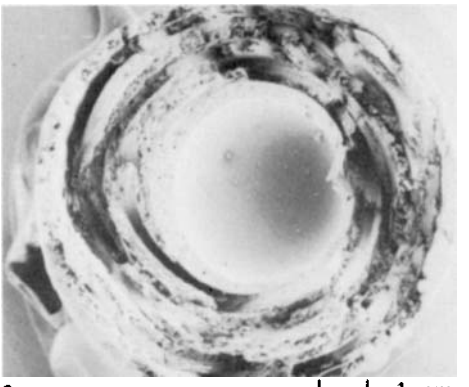

2 1 mm

3 200 μm

4 20 μm

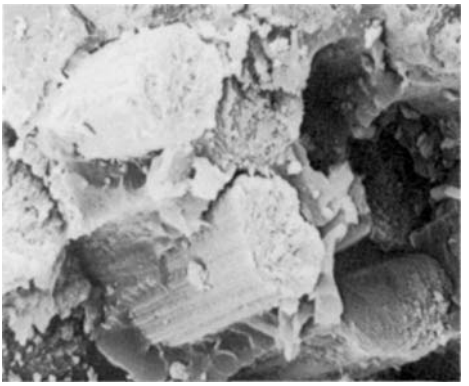

5 5 μm

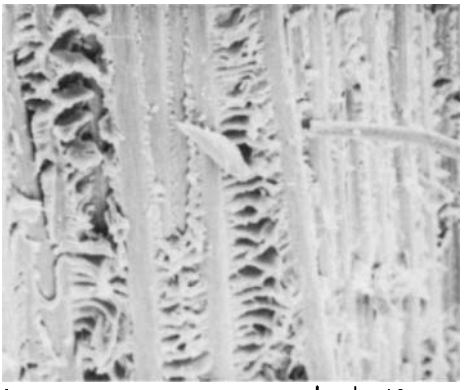

6 10 μm

Plate 40D — Breakage of the shaft of a badminton racket made from a carbon fibre composite.
(1) Photograph of fracture. (2) End-on view of fracture. (3)–(6) Detail of breakage.

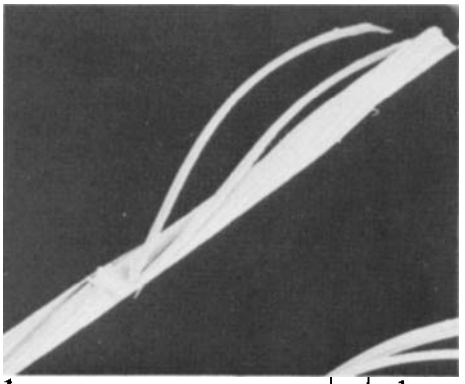

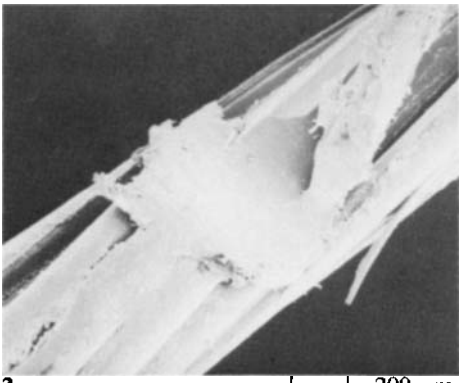

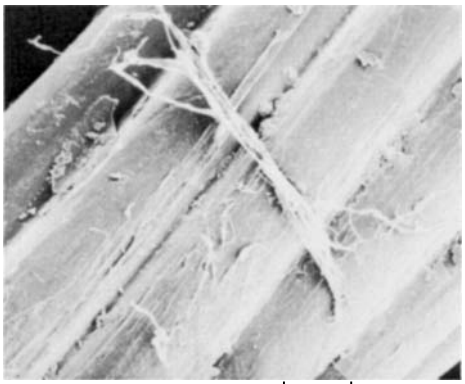

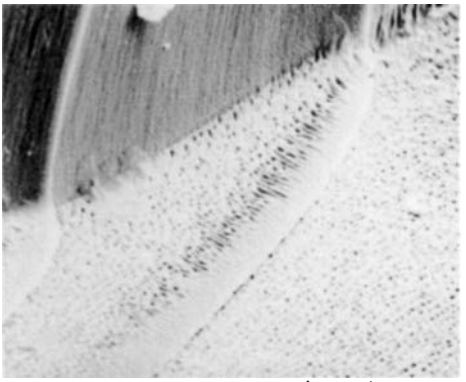

Plate 40E — Broken string of badminton racket.
(1) General view of break. (2) Cross-over point of strings. (3) Peeling on string surface, due to general wear at centre of racket. (4)–(6) Detail of break.

1 ⊢⊣ 1 mm

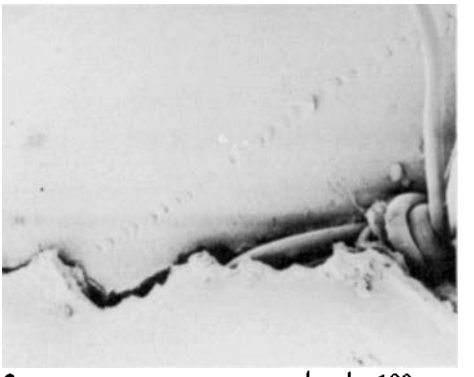

2 ⊢⊣ 100 μm

3 ⊢⊣ 50 μm

4 ⊢⊣ 50 μm

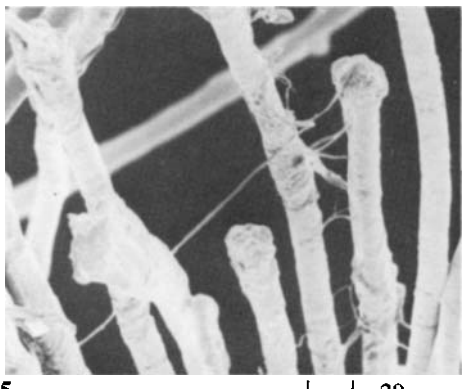

5 ⊢⊣ 20 μm

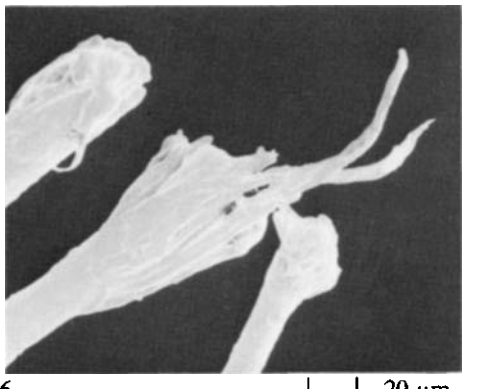

6 ⊢⊣ 20 μm

Plate 40F — Break of tennis racket string.
(1) General view of break. (2) Detail of damage to sheath. (3),(4) Fibre breaks.

Break of one strand of archery bowstring.
(5) Fibres near break. (6) Detail of breakage.

1 ⊢⊣ 20 μm

2 ⊢⊣ 20 μm

3

4 ⊢⊣ 5 μm

5 ⊢⊣ 1 mm

6 ⊢⊣ 50 μm

Plate 40G — Four forms of fibre damage.
(1),(2) Nylon 6 monofil used to transport sheets through an automatic laundry, after 10 hours service. (3) Nylon filament removed from worn tyre; optical micrograph, from S. C. Simmens. (4) Break in nylon filament from a parachute cord, deployed during aircraft landing. (5),(6) Hole in polypropylene fabric, which had been used to filter china clay.

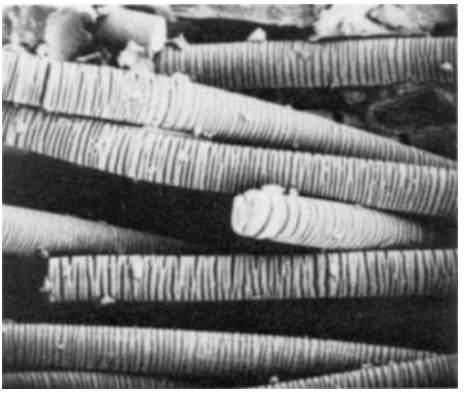

1

2

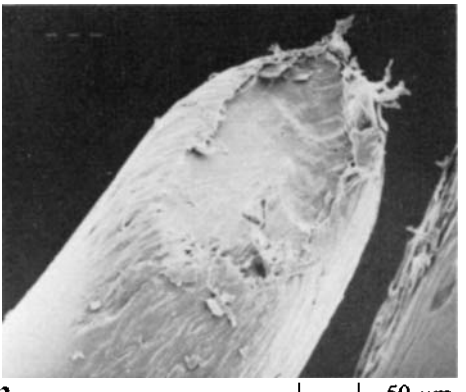

3 50 μm

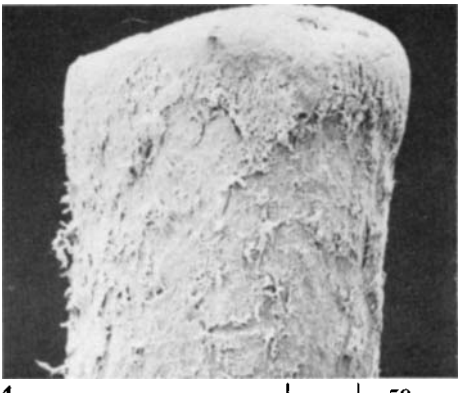

4 50 μm

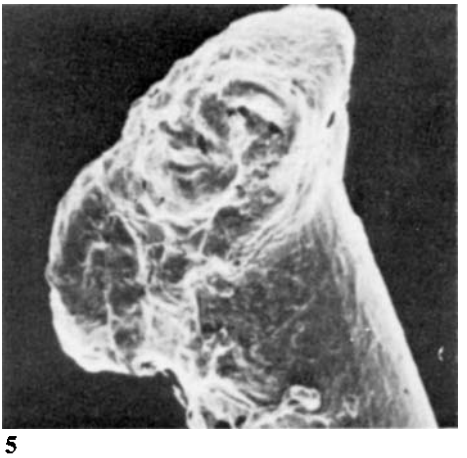

5

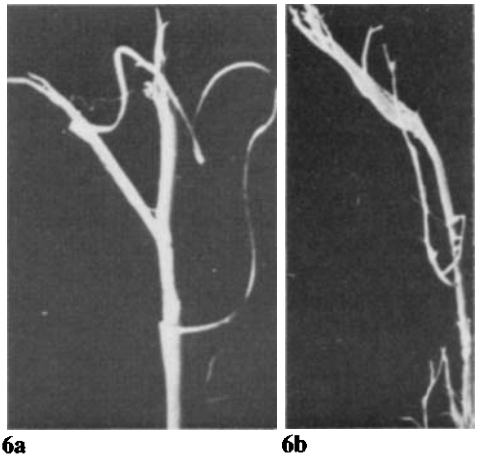

6a 6b

Plate 40H — Polypropylene fabric after five years exposure to light in a cover on the back seat of a car.
(1) Filaments with transverse cracks. (2) Internal appearance after splitting open.

Toothbrush, Oral 30B.
(3) Bristle in new brush. (4) Bristle in used brush.

Ballistic impact resistance.
(5) From nylon fabric, impacted by bullet at 514 m/s. (6) From Kevlar fabric, impacted at: (a) 240 m/s; (b) 523 m/s.

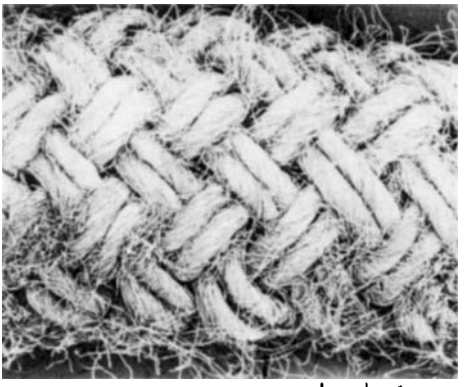

1 ⊢⊣ 1 mm

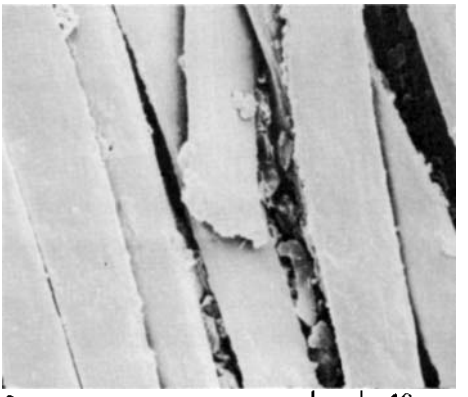

2 ⊢⊣ 10 μm

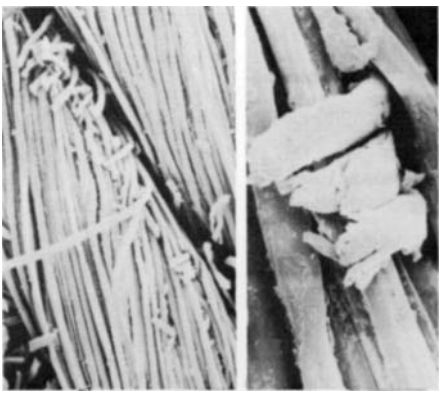

3a ⊢⊣ 100 μm 3b ⊢⊣ 10 μm

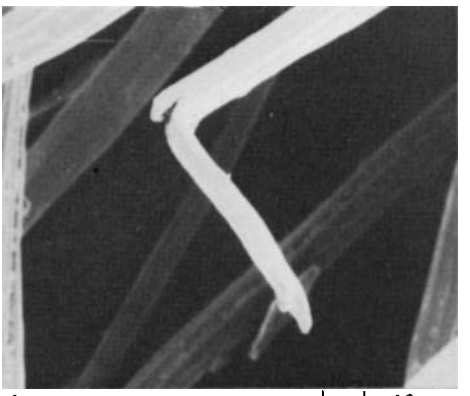

4 ⊢⊣ 10 μm

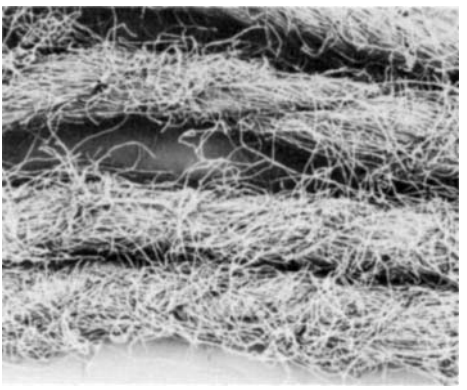

5 ⊢⊣ 1 mm

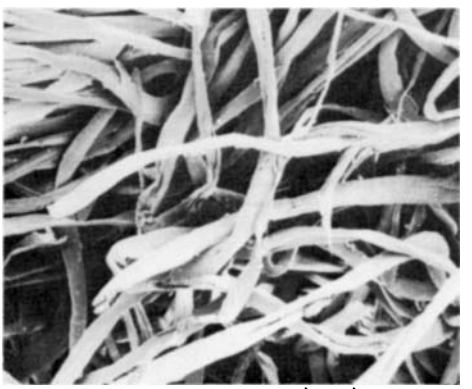

6 ⊢⊣ 500 μm

Plate 40I — Broken shoe-lace.
(1) Surface of outer braid, near the break. (2) Surface wear and break of rayon fibres in braid. (3a, b) Broken fibres in braid. (4) Rayon break, close to break in lace. (5) Exposed cotton yarns from core. (6) Detail of cotton fibre damage.

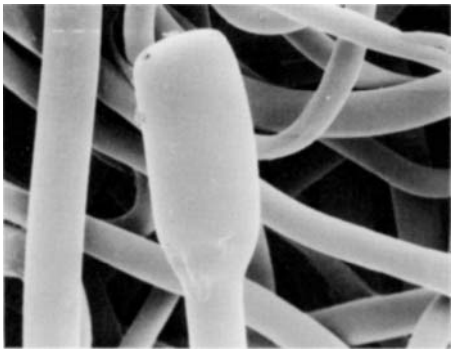

1

2

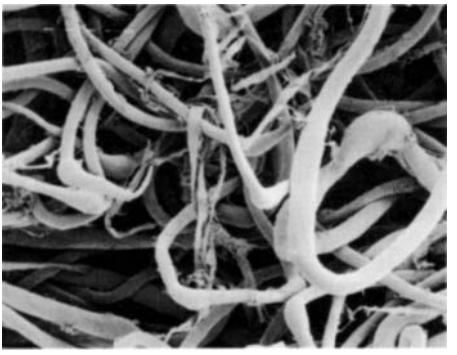

3

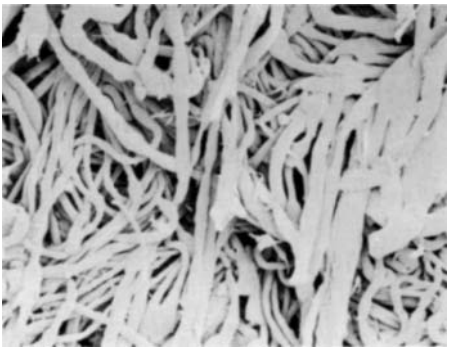

4

5

6

Plate 40J — Wear in papermakers' felts.
(1) Unused felt. (2) Used felt. (3)–(6) Part used felts.

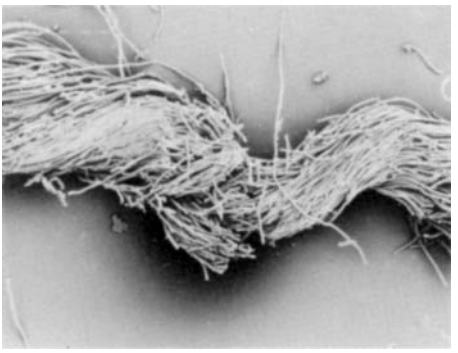

1

2

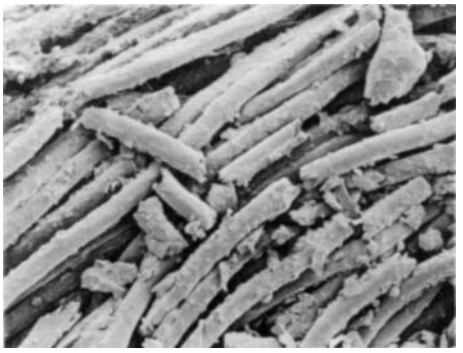

3

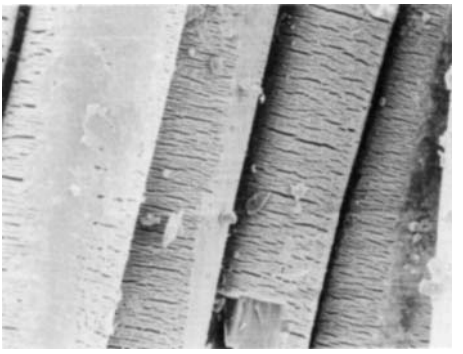

4

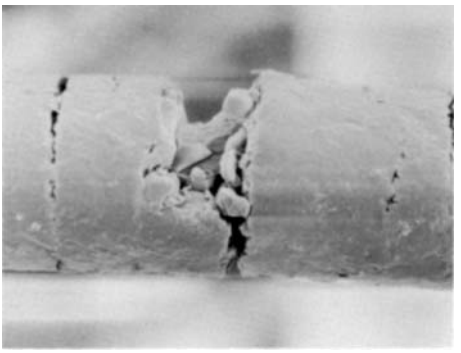

5

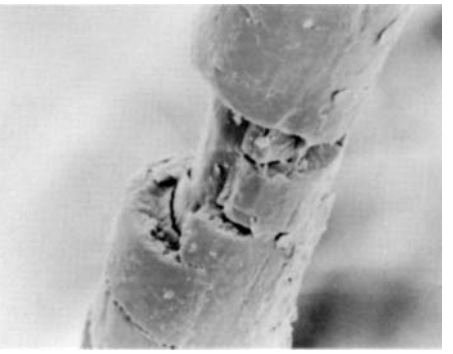

6

Plate 40K — A degraded polypropylene filter.
(1) Yarn breaking. (2) Details of fibre breaks. (3) General damage. (4) Transverse cracks and pieces breaking off.

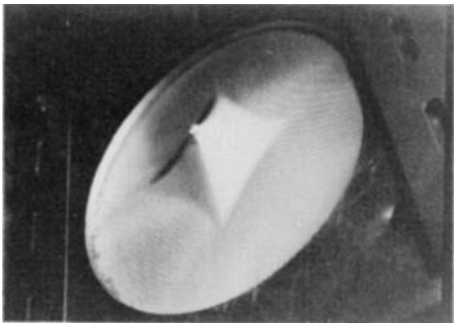

1

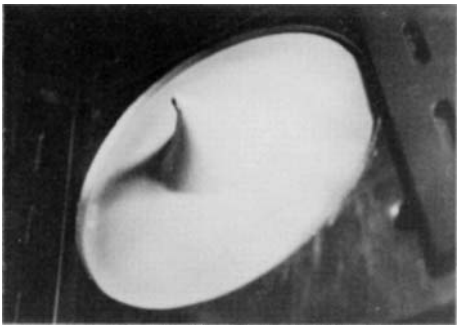

2

3

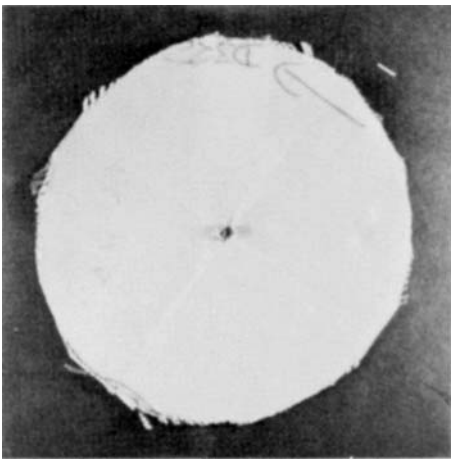

4

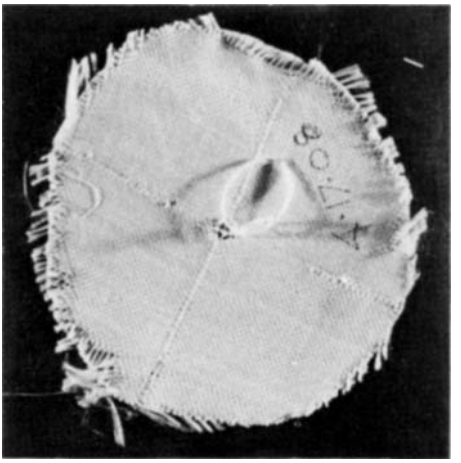

5

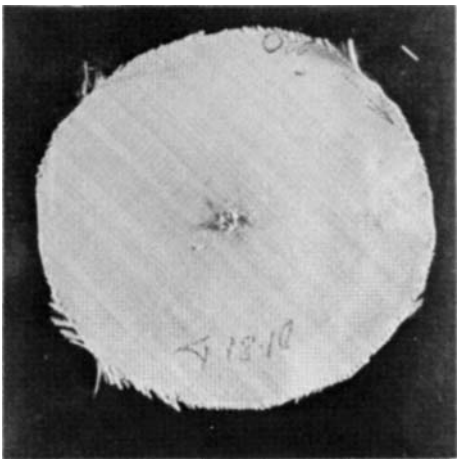

6

Plate 40L — Ballistic impact.
(1) Penetration of woven nylon fabric. (2) Penetration of knit nylon fabric. (3) Residual damage after impact on nylon fabric at 254 m/s. (4) After impact at 514 m/s. (5) Kevlar fabric after impact at 240 m/s. (6) After impact at 554 m/s.